JOURNAL OF GEOPHYSICAL RESEARCH, VOL. 98, NO. B11, PAGES 19,835–19,858, NOVEMBER 10, 1993

The 1992 Landers Earthquake Sequence: Seismological Observations

EGILL HAUKSSON,[1] LUCILE M. JONES,[2] KATE HUTTON,[1] AND DONNA EBERHART-PHILLIPS[2]

The (M_W6.1, 7.3, 6.2) 1992 Landers earthquakes began on April 23 with the M_W6.1 1992 Joshua Tree preshock and form the most substantial earthquake sequence to occur in California in the last 40 years. This sequence ruptured almost 100 km of both surficial and concealed faults and caused aftershocks over an area 100 km wide by 180 km long. The faulting was predominantly strike slip and three main events in the sequence had unilateral rupture to the north away from the San Andreas fault. The M_W6.1 Joshua Tree preshock at 33°N58' and 116°W19' on 0451 UT April 23 was preceded by a tightly clustered foreshock sequence (M≤4.6) beginning 2 hours before the mainshock and followed by a large aftershock sequence with more than 6000 aftershocks. The aftershocks extended along a northerly trend from about 10 km north of the San Andreas fault, northwest of Indio, to the east-striking Pinto Mountain fault. The M_W7.3 Landers mainshock occurred at 34°N13' and 116°W26' at 1158 UT, June 28, 1992, and was preceded for 12 hours by 25 small M≤3 earthquakes at the mainshock epicenter. The distribution of more than 20,000 aftershocks, analyzed in this study, and short-period focal mechanisms illuminate a complex sequence of faulting. The aftershocks extend 60 km to the north of the mainshock epicenter along a system of at least five different surficial faults, and 40 km to the south, crossing the Pinto Mountain fault through the Joshua Tree aftershock zone towards the San Andreas fault near Indio. The rupture initiated in the depth range of 3-6 km, similar to previous M~5 earthquakes in the region, although the maximum depth of aftershocks is about 15 km. The mainshock focal mechanism showed right-lateral strike-slip faulting with a strike of N10°W on an almost vertical fault. The rupture formed an arclike zone well defined by both surficial faulting and aftershocks, with more westerly faulting to the north. This change in strike is accomplished by jumping across dilational jogs connecting surficial faults with strikes rotated progressively to the west. A 20-km-long linear cluster of aftershocks occurred 10-20 km north of Barstow, or 30-40 km north of the end of the mainshock rupture. The most prominent off-fault aftershock cluster occurred 30 km to the west of the Landers mainshock. The largest aftershock was within this cluster, the M_W6.2 Big Bear aftershock occurring at 34°N10' and 116°W49' at 1505 UT June 28. It exhibited left-lateral strike-slip faulting on a northeast striking and steeply dipping plane. The Big Bear aftershocks form a linear trend extending 20 km to the northeast with a scattered distribution to the north. The Landers mainshock occurred near the southernmost extent of the Eastern California Shear Zone, an 80-km-wide, more than 400-km-long zone of deformation. This zone extends into the Death Valley region and accommodates about 10 to 20% of the plate motion between the Pacific and North American plates. The Joshua Tree preshock, its aftershocks, and Landers aftershocks form a previously missing link that connects the Eastern California Shear Zone to the southern San Andreas fault.

INTRODUCTION

The Landers earthquake sequence is the largest sequence recorded by the Southern California Seismographic Network since monitoring began in the 1920s. The sequence extended over an area of 100 km by 180 km. In addition to the aftershocks within one fault length distance of the (M_W7.3) Landers earthquake rupture, an increase in seismicity at greater distances in southern California and along the volcanic belt in eastern California was reported following the mainshock (*Hill et al., 1993*).

The 1992 Landers and Joshua Tree earthquakes occurred in the Eastern California Shear Zone (ECSZ) (Figure 1). The ECSZ extends northwestward from the southern San Andreas fault zone into the central Mojave Desert, near Barstow, where it turns to the north-northwest into the Death Valley region [*Dokka and Travis,* 1990a]. In the central and eastern Mojave Desert the ECSZ consists of several major strike-slip faults that strike north to northwest. The mapped surface traces of these faults extend from the Pinto Mountain fault in the south, across the central and eastern Mojave Desert, to the Garlock fault in the north [*Dibblee,* 1967; *Dokka,* 1983]. Individually these faults all have low slip rates of <1.0 mm/yr [*Dokka,* 1983; *Dokka and Travis,* 1990b], but the total strain rate of the ECSZ from geologic and geodetic data is about 8 mm/yr [*Sauber et al.,* 1986; *Savage et al.,* 1990]. The ECSZ transfers some of the relative motion between the North American-Pacific plates away from the dominant plate boundary structure, the San Andreas fault zone, to the western Great Basin of the Basin and Range province. Sixty years of earthquake monitoring (1930-1992) have shown significant microseismicity in the Mojave Desert. Several moderate earthquakes have also been recorded in the Mojave with the previous largest event, the 1947 M6.5 Manix earthquake.

The 1992 Landers sequence occurred along the western edge of the ECSZ. Previously, *Hadley and Kanamori* [1977] suggested that the active plate boundary at depth between the North American and Pacific Plates was along

[1]Seismological Laboratory, Division of Geological and Planetary Science, California Institute of Technology, Pasadena.
[2]U.S. Geological Survey, Pasadena, California.

Paper number 93JB02384.
0148-227/93/93JB-02384$05.00

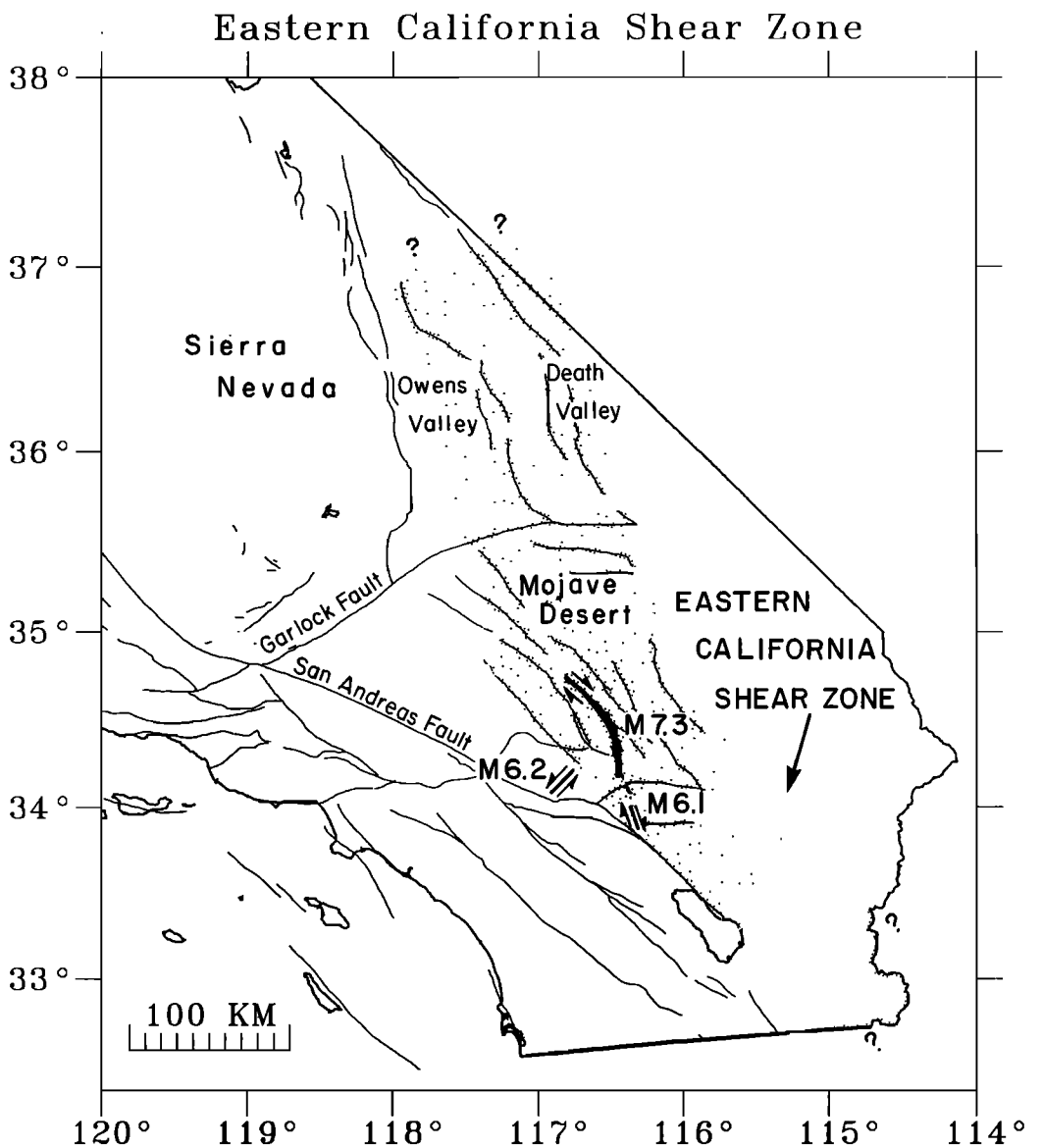

Fig. 1. Map of the Eastern California Shear Zone (ECSZ) [*Dokka and Travis*, 1990b] showing major faults from *Jennings* [1975] and the locations of the M_W6.1 Joshua Tree, M_W7.3 Landers, and M_W6.2 Big Bear earthquakes.

the western edge of the ECSZ or in the vicinity of the Helendale-Lenwood-Camp Rock faults. Furthermore, geological observations by *Dokka and Travis* [1990b] showed that tectonic activity has migrated from east to west across the ECSZ during the last 5-10 Ma. The occurrence of the Landers sequence thus is consistent with geological, geophysical, and geodetic data from the region.

This paper analyzes the details of the earthquakes in the Landers sequence. To describe this large sequence, we separate it into (1) the Joshua Tree sequence (events before June 28), (2) the immediate foreshocks and the Landers mainshock, (3) aftershocks south of the mainshock epicenter, (4) aftershocks occurring along the mainshock rupture, (5) aftershocks along the Calico and Pisgah faults, (6) the Barstow sequence, and (7) the Big Bear sequence. We also examine the temporal and magnitude distribution of the sequence. The aftershocks illuminate numerous seismotectonic structures of the Mojave Desert and the San Bernardino Mountains. Many of these structures are being imaged for the first time, facilitating our understanding of the role these structures play in plate-boundary deformation.

DATA AND LOCATION PROCEDURES

We analyzed the *P* and *S* arrival times and *P* wave first-motion data from the Southern California Seismic Network (SCSN), operated by the U.S. Geological Survey and the California Institute of Technology (USGS/CIT), to obtain high-quality hypocenters and focal mechanisms. The SCSN recorded approximately 6000 Joshua Tree aftershocks and 40,000 Landers aftershocks. All of the Joshua Tree data and data from about 20,000 Landers aftershocks are available for this study. This data set is somewhat incomplete at magnitude (M) less than 3 for the months of June, July, and August 1992 because data processing is ongoing. Arrival time data from two explosions detonated in the Landers area [*Eberhart-Phillips et al.*, 1992] and several previous explosions [*Kanamori*

and Fuis, 1976] and 276 earthquakes were simultaneously inverted for improved hypocenters, two velocity models, and a set of station delays using the VELEST code [*Roecker and Ellsworth*, 1978]. Arrival time data were used from the stations shown in Figure 2. An initial model from *Hadley and Kanamori* [1977] was used as a starting regional model in the inversion, and a separate velocity model was assigned to stations located within 50 km of the Landers fault rupture. The starting and final velocity models are listed in Table 1. The resultant models and delays were used as input to HYPOINVERSE [*Klein*, 1985] to obtain final locations for both sequences, which included more than 26,000 events. When the two blasts were relocated using the new models and station delays, their location shifted less than 0.5 km away from the true location. The relative vertical and horizontal uncertainties in the hypocenters are in most cases less than 1 km. The initial starting depth for all of the events was chosen to be 8 km. A few hypocenters remain at the 8 km depth because the arrival time data are insufficient to constrain their depth. The final locations on the average had a root-mean-square residual (rms) of 0.10 s as compared with the rms of 0.25 s when using the starting model.

More than 2000 single-event, lower hemisphere focal mechanisms were determined using the grid-searching algorithm and computer programs by *Reasenberg and Oppenheimer* [1985]. The uncertainties in the strike, dip, and rake of the focal mechanisms are on the average for the whole data set 10°, 24°, and 25° (E. Hauksson, State of stress from focal mechanisms before and after the 1992 Landers earthquake sequence, submitted to *Bulletin of the Seismological Society of America, 1993*). To provide an overview of the sequence only a few typical focal mechanisms for the large events are shown in the figures. Sample focal mechanisms with first-motion polarities for $M \geq 5$ events are shown in Figure 3 and listed in Table 2.

SEISMOLOGICAL OBSERVATIONS

Overview

The dominance of strike-slip motion is one of the main characteristics of the Landers earthquake sequence. The Joshua Tree earthquake, the first major event in the Landers sequence, resulted from right-lateral strike-slip faulting in a N20°W direction. The first motion focal mechanism of the Landers mainshock that was located north of the Pinto Mountain fault had a more northerly direction of N10°W

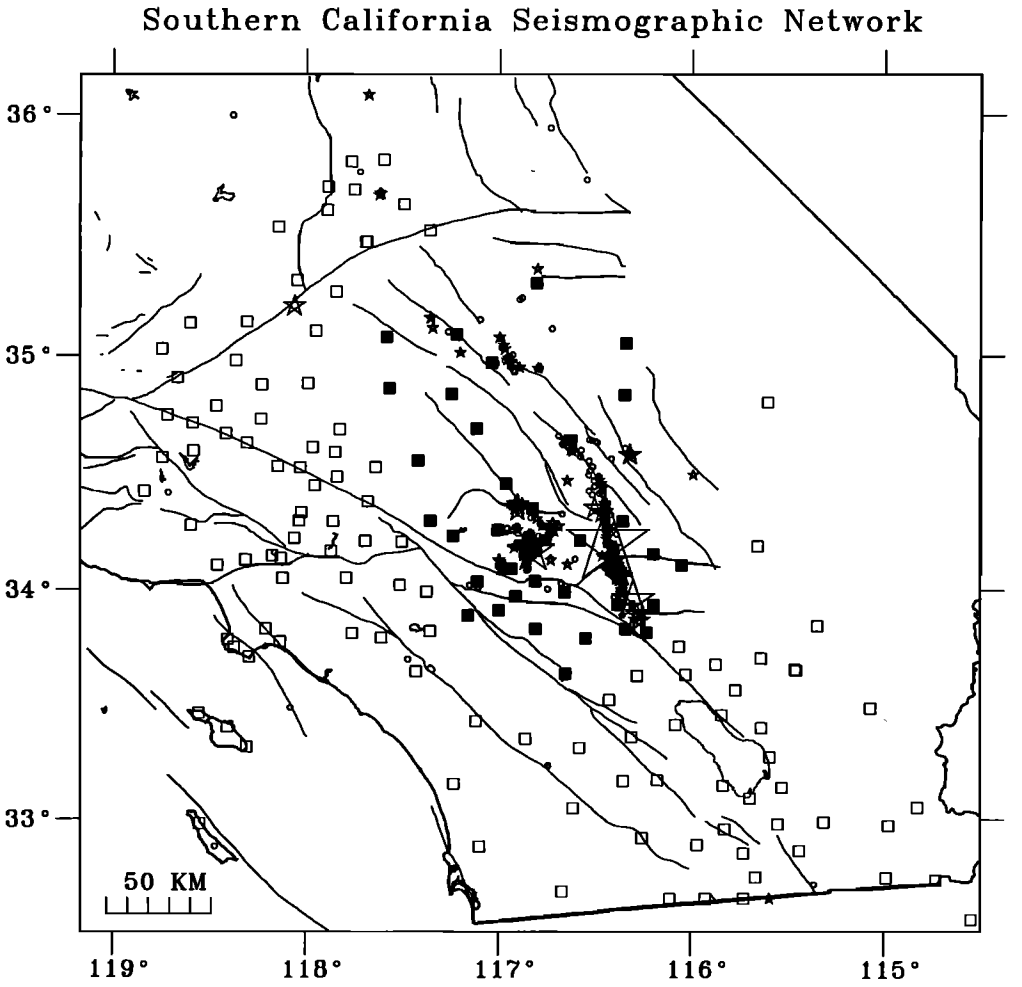

Fig. 2. Map of the southern California Seismographic Network (SCSN). Seismic stations are shown by squares. Solid squares are stations that were assigned the Landers velocity model, and open squares are stations assigned the southern California velocity model in Table 1. Earthquakes of $M \geq 3.5$ recorded from June to December 1992 by SCSN are included, shown as stars for M≥4 and circles for $M < 4$.

TABLE 1. *P* Wave Velocity Models

Initial Velocity km/s	Refined Velocity, km/s	Depth to Top of Layer, km
Southern California Model		
4.30	3.74	0.00
5.80	5.82	2.00
6.10	6.23	5.50
6.70	6.60	16.0
7.80	7.63	32.0
Landers Model		
4.30	4.54	0.00
5.50	5.84	2.00
5.80	6.13	5.50
6.70	6.56	16.0
7.80	7.80	32.0

(Figure 4). The Joshua Tree and Landers earthquakes created their own abutting aftershocks zones as well as a northern off-fault cluster of aftershocks, the Barstow sequence. The Barstow sequence is separated by 30-40 km from the north end of the Landers mainshock rupture. Another off-fault aftershock cluster located 30-40 km west of the mainshock in the San Bernardino Mountains, the Big Bear sequence, showed left-lateral strike-slip faulting on northeast striking planes. Both the Barstow and Big Bear sequences occurred within a distance less than one rupture length of the Landers mainshock, and thus we consider both sequences as aftershocks of the Landers earthquake.

The Landers sequence has generated 13 earthquakes of M>5.0 as of July 1, 1993. Large aftershocks of M≥4.0 are most common south of the Landers epicenter and in the Big Bear aftershock zone (Figure 5). The first (M5.8) and second (M5.6) large aftershocks 3 and 4 min after the mainshock are located at the north and south ends of the Eureka Peak fault, respectively. The southern cluster of large aftershocks occurs near the Eureka Peak and Burnt Mountain faults, and extends across the Joshua Tree aftershock zone further south to the San Andreas fault where an M5.0 event and an M5.2 event occurred. The several large aftershocks that occurred in the Big Bear area are not clearly associated with mapped faults.

The six faults involved in the Landers mainshock rupture had relatively few large (M>4.5) aftershocks, with the most located to the south of the mainshock epicenter (Figure 5). This variation in the spatial distribution of large aftershocks is reflected in the b value of the sequence. The b value of the total sequence is 0.95, the b value for Big Bear and the region south of the mainshock is 0.87, and the mainshock and Barstow region have a b value of 1.05. The lack of large aftershocks along the Homestead Valley, Emerson, and Camp Rock faults coincides with regions of large slip in the mainshock estimated from seismic recordings [*Kanamori et al.*, 1992], as well as regions of extensive mapped surface rupture with offsets on the order of meters [*Sieh et al.*, 1993].

Strike slip is also the dominating mode of deformation in the large aftershocks (Figure 5). Only two M≥5 events, both in the San Bernardino Mountains, showed thrust faulting. The August 17 event, at a depth of 13 km, cannot

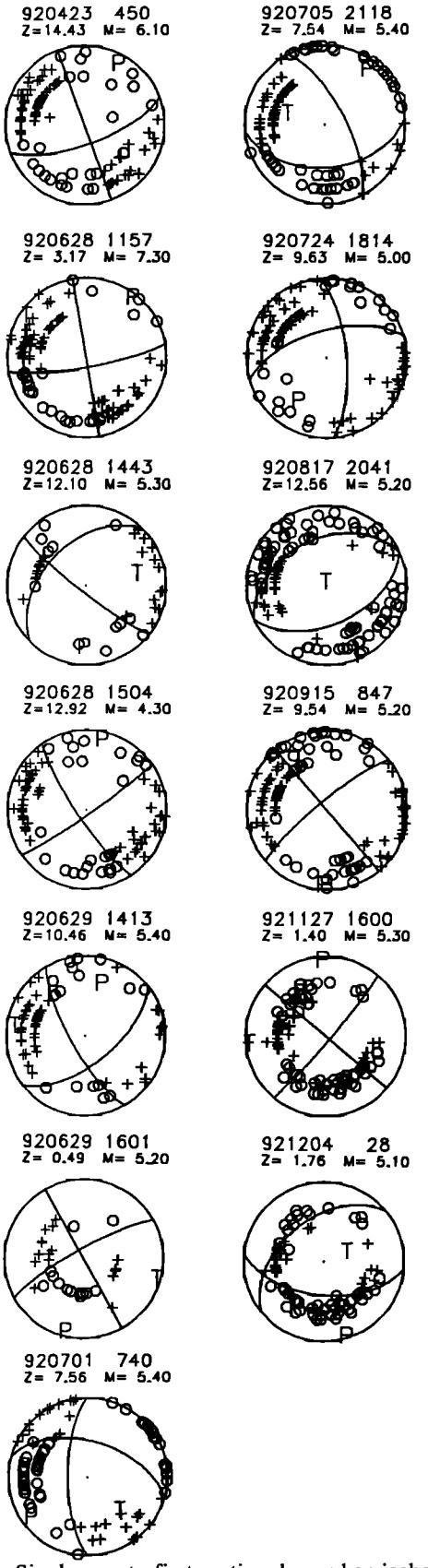

Fig. 3. Single-event, first-motion lower-hemisphere focal mechanisms of selected M≥5 events. Compressional first motions are shown by pluses and dilational first motions by open circles. The first motions of the M6.2 Big Bear event were obscured by its immediate foreshock (M4.3) which is shown here.

TABLE 2. Locations and Focal Mechanisms of Earthquakes in the 1992 Landers Sequence

Origin Date	Time, UT	Latitude N	Longitude W	Depth, km	Mag M_L	Focal Mechanisms Ddir	Dip	Rake	Number of First Motions
April 23, 1992	0450	33°57.33'	116°17.97'	14.4	6.1	70°	90°	160°	91
June 28, 1992	1157	34°12.13'	116°25.95'	3.2	7.3	80°	90°	170°	71
June 28, 1992	1443	34°09.96'	116°51.34'	12.1	5.3	315°	45°	10°	23
June 28, 1992	1505	34°09.94'	116°49.35'	12.9	6.2	145°	85°	-10°	86*
June 29, 1992	1413	34°06.21'	116°23.99'	10.5	5.4	240°	75°	-150°	51
June 29, 1992	1601	33°52.11'	116°16.09'	0.5	5.2	330°	80°	0°	48
July 1, 1992	0740	34°20.01'	116°27.59'	7.6	5.4	270°	70°	140°	63
July 5, 1992	2118	34°34.81'	116°19.10'	7.5	5.4	175°	45°	30°	54
July 24, 1992	1814	33°53.88'	116°16.88'	9.6	5.0	85°	70°	-150°	78
Aug. 17, 1992	2041	34°11.71'	116°51.63'	12.6	5.2	155°	50°	90°	93
Sept. 15, 1992	0847	34°03.64'	116°21.50'	9.5	5.2	50°	90°	-170°	78
Nov. 27, 1992	1600	34°20.54'	116°54.20'	1.4	5.3	130°	85°	0°	87
Dec. 04, 1992	0028	34°21.98'	116°54.19'	1.8	5.1	185°	55°	120°	94

*The focal mechanism of the foreshock that preceded this event by 40 s is shown in Figure 3.

be associated with any mapped faults. The December 4 event, at a depth of 2 km, probably occurred on the North Frontal fault zone (NFFZ) of the San Bernardino Mountains.

The 1992 Joshua Tree Sequence

The Landers earthquake sequence began with the M_W6.1 Joshua Tree earthquake of April 23, 1992, 0450 UT at 33°N57.3', 116°W18.0', 10 km east of the southern San Andreas fault and 20 km south of the Pinto Mountain fault (Figure 6). It nucleated at a depth between 12 and 15 km. The earthquake was preceded by seven foreshocks, beginning with an M_L4.6 event at 0225 UT. The mainshock was followed by over 6000 aftershocks by June 28. No definitive tectonic surface rupture for the sequence was found [*Rymer*, 1992].

The locations of the mainshock and aftershocks suggest that the Joshua Tree mainshock ruptured unilaterally to the north along a fault about 10-14 km long. *P* wave polarities indicate right-lateral slip initiated on a fault striking N20°W, dipping 90°, with a rake of 160°. Well-located aftershocks form an almost vertical aftershock zone (Figure 6).

A large number of aftershocks occurred off the mainshock rupture plane on adjacent secondary structures, similar to the conjugate pattern of events following the 1979 M_L 5.3 Homestead Valley earthquake [*Hutton et al.*, 1980]. In the case of the 1979 earthquake, *Stein and Lisowski* [1983] showed that these off-fault aftershock clusters occurred preferentially where the mainshock dislocation had raised the calculated shear stress by at least 0.3MPa. Many of the Joshua Tree off-fault aftershocks had right-lateral focal mechanisms with nodal planes either subparallel to the mainshock plane or auxiliary nodal planes striking at high angles. Because the off-fault aftershock clusters in most cases have cylindrical shapes, it is not easy to differentiate between the two possible nodal planes.

The aftershock zone extended to the north and south during the first days following the mainshock, and ultimately extended from the southern San Andreas fault near the Indio Hills to the Pinto Mountain fault (Figure 7). In April the southern half of the zone had a N20°W trend while the northern half trended north. The focal mechanisms along the aftershock zone agree with the varying strike inferred from the seismicity pattern. Some scattered activity also occurred north of the Pinto Mountain fault. In May the north trend became more prominent than before and a conjugate, east-west trend continued to develop at latitude 34°-34°2'. In early June two dense clusters of earthquakes occurred north of the Pinto Mountain fault. A third cluster began 12 hours before the Landers mainshock, at the mainshock epicenter. These immediate Landers foreshocks are also shown in Figure 7. Although Joshua Tree aftershocks occurred on many different small faults, none could be associated with the Pinto Mountain or Blue Cut faults.

The 1992 Joshua Tree sequence occurred in an area of frequent earthquake swarms. The 1940 M_L5.3 Covington Flats earthquake that was part of the precursory activity to the 1948 M_W6.0 Desert Hot Springs event may have occurred just north of the 1992 Joshua Tree earthquake [*Richter et al.*, 1958; *Sykes and Seeber*, 1985; C. Nicholson, written communication, 1992]. The predominance of swarms and the many faults activated by the Joshua Tree aftershocks suggest that the faults in this region are not well developed.

Foreshocks and Landers Mainshock

At least 25 immediate foreshocks of M1.3-3.0 occurred during the 7 hours preceding the Landers mainshock (Figure 8). These foreshocks, ranging in depth from near surface to 4 km, were located within an area of 1.5 km diameter, forming a tight spatial cluster at and mostly south of the mainshock epicenter.

Although the foreshocks were densely clustered in time and space and appear to be both spatially and temporally related to the occurrence of the mainshock, they were not considered anomalous at the time of their occurrence. They were small ($M \leq 3.0$) and were located within the northern edge of the expanding aftershock zone of the 1992 M_W6.1 Joshua Tree earthquake. The only difference from the other aftershock clusters that occurred north of the Pinto Mountain fault in June was that the foreshocks were more

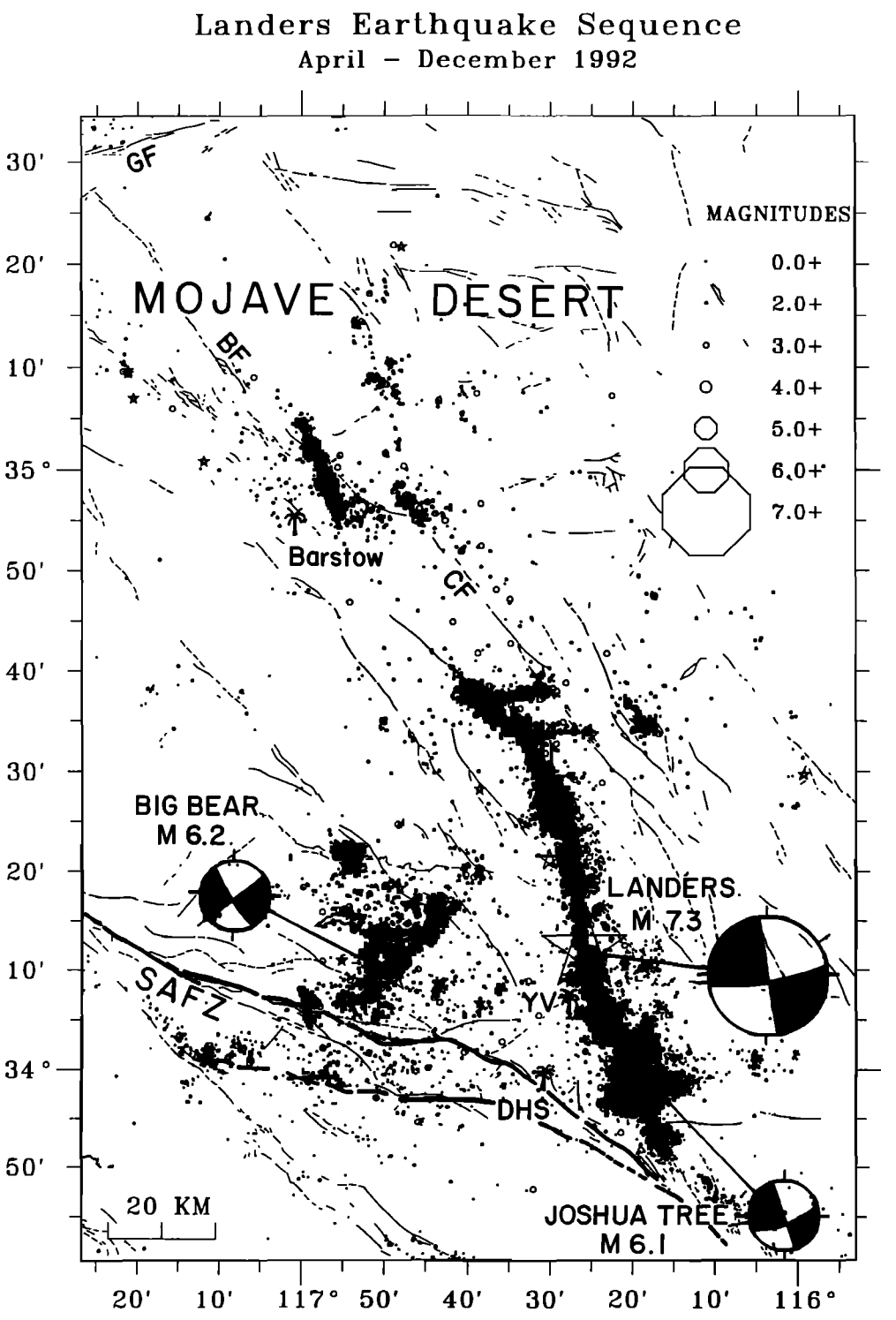

Fig. 4. Landers aftershock region showing all earthquakes recorded by the SCSN from April to December 1992, and major faults (dotted if inferred) from *Jennings* [1975]. Lower-hemisphere, first-motion focal mechanisms, compressional quadrant shaded, of the three main earthquakes are also shown. BF, Blackwater fault, CF, Calico fault, YV, Yucca Valley, GF, Garlock fault, SAFZ, San Andreas fault zone, and DHS, Desert Hot Springs. Earthquakes of $M \geq 4.0$ are shown by stars.

tightly clustered in space [*Mori and Jones*, 1992], but this is not very unusual for earthquakes of this small magnitude range.

The M_W7.3 Landers mainshock occurred at 1157 UT on June 28, 1992. The mainshock epicenter, at 34°12.1'N 116°25.9'W, and at a depth of 3-6 km locates 0.5 km east of the mapped trace of the Johnson Valley fault, 8 km south-southwest of the town of Landers. The mainshock depth is uncertain because no nearby *S* arrival times are available and the distance to the closest station was 13 km. The first motion focal mechanism of the mainshock showed almost pure right-lateral strike slip with a nodal

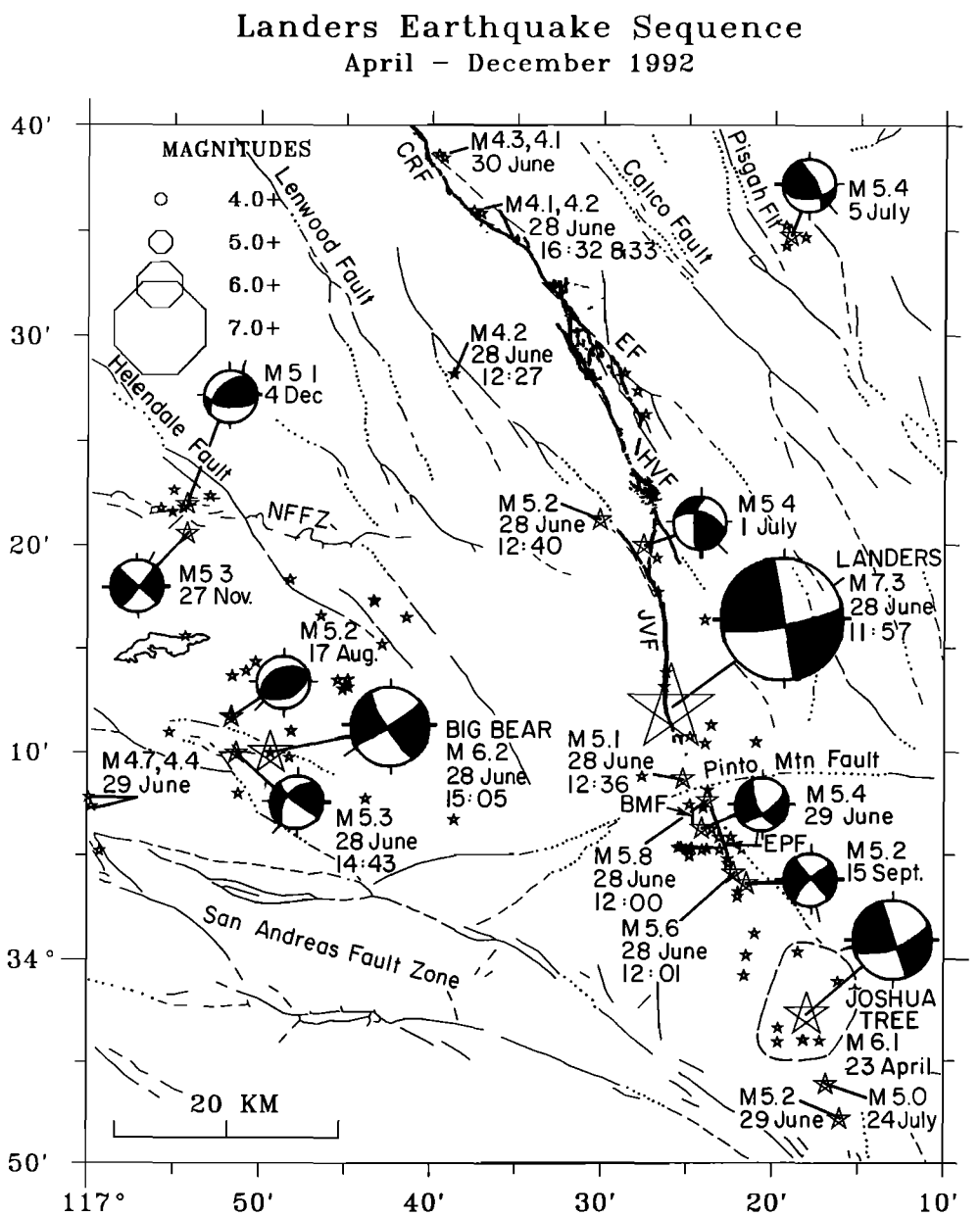

Fig. 5. Landers aftershock region showing all earthquakes recorded by the SCSN of $M \geq 4.0$ from April to December 1992, and major faults (dotted if inferred) from *Jennings* [1975]. Heavy line represents surface rupture. Joshua Tree earthquakes (April 22- June 28) are enclosed by a dashed curve. Lower-hemisphere, first-motion focal mechanisms of the $M>5$ events are also shown. CRF, Camp Rock fault; EF, Emerson fault; JVF, Johnson Valley fault; NFFZ, North Frontal fault zone; BMF, Burnt Mountain fault, EPF, Eureka Peak fault, HVF, Homestead Valley fault.

plane striking N10°W, rake of -170°, and dip of 90°, which is almost identical to the focal mechanism determined from teleseismic data [*Kanamori et al.*, 1992]. The northerly striking nodal plane, with almost the same strike as the Johnson Valley fault (Figure 5), projects up to the surface less than 0.5 km east of the surface trace of that fault. The difference may indicate the absolute accuracy of the mainshock epicenter or possible geometrical complexities in the Johnson Valley fault. If the depth of the mainshock is assumed to be greater than 6 km, the first motion focal mechanism exhibits a significant normal component, which was not observed in the surface rupture or the long-period focal mechanism [*Sieh et al.*, 1993].

The interpretations of teleseismic data show two major subevents with depth of faulting extending down to 15 km [*Wald et al.*, 1992; *Kanamori et al.*, 1992]. The mainshock started slowly and most of the teleseismic models [e.g., *Wald et al.*, 1992, *Thio and Kanamori*, 1992] of the mainshock require about a 3-s delay in the onset of the main energy release in the first subevent. An initial, smaller subevent comparable to an $M4$-5 earthquake appears to be the location of the Landers mainshock determined from arrival times from the SCSN [*Abercrombie et al.*, 1992]. Previous $M5$ events in the Mojave Desert have been confined to the upper crust, above 5 km [*Hutton et al.*, 1980; *Lindh et al.*, 1978]. The

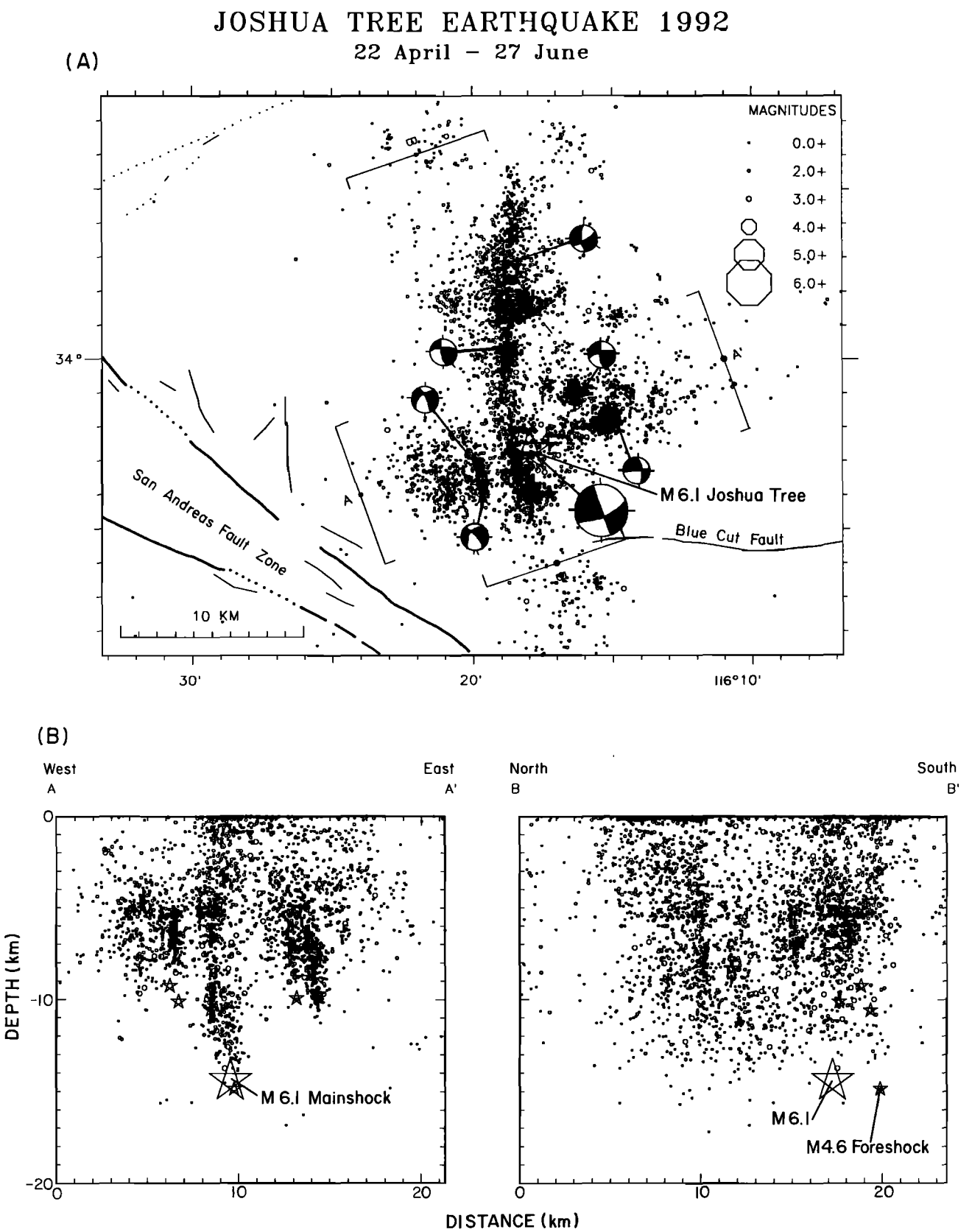

Fig. 6. (a) The M_W6.1 1992 Joshua Tree earthquake sequence. Typical lower hemisphere focal mechanisms are shown for the mainshock and a few large aftershocks. (b) Cross sections parallel and orthogonal to the mainshock fault showing the depth distribution of the aftershocks. Earthquakes of $M \geq 4.0$ are shown by stars.

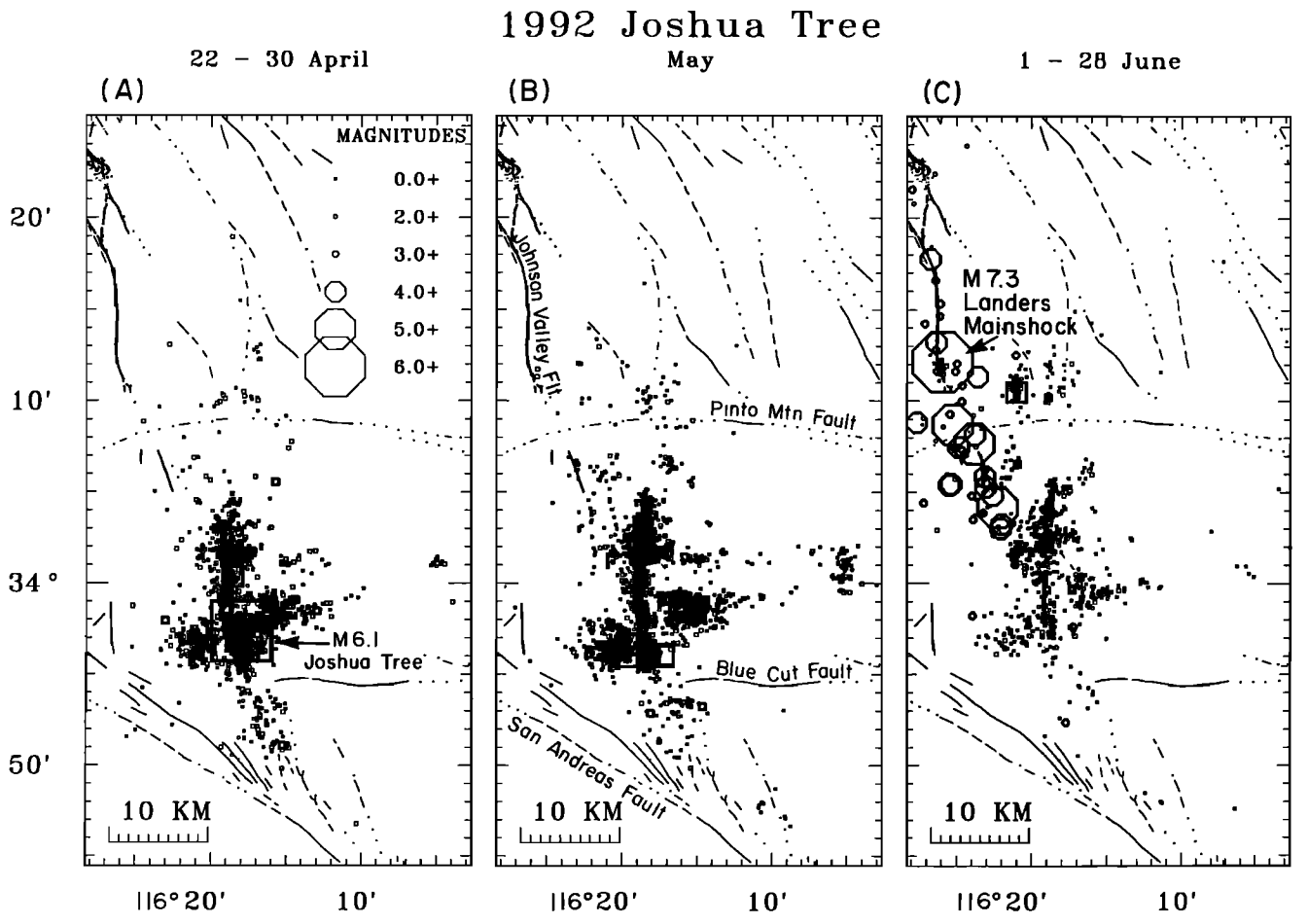

Fig. 7. Spatial and temporal development of the M_W6.1 1992 Joshua Tree sequence. (a) Foreshocks, mainshock, and aftershocks that occurred during April 22-30, 1992. (b) Aftershocks during May 1992. (c) Aftershocks during June 1-28, 1992, and the M_W7.3 Landers foreshocks (squares) and the Landers aftershocks (octagons) that occurred during the first 12 hours of aftershock activity on June 28.

shallow depth of the mainshock hypocenter and the delay in energy release suggest that the Landers mainshock began as a shallow, moderate earthquake that within a few seconds triggered a larger, deeper event.

Seismic Zone South of Landers

A 5-to 15-km-wide zone of aftershocks extends 40 km south of the epicenter of the Landers mainshock (Figure 9). This zone strikes north-northwest and crosses the Pinto Mountain fault, the previous Joshua Tree aftershock zone, and the Blue Cut fault, and terminates within a few kilometers of the San Andreas fault near Indio. It includes many small and large (M>4.0) aftershocks, including the first two large aftershocks of M5.8 and M5.6 (Figure 5). The strike of this zone corresponds to the strike of the Joshua Tree focal mechanism but differs distinctly from the northern pattern of the Joshua Tree aftershock zone.

Typical focal mechanisms of aftershocks from within this zone are also shown in Figure 9. The style of faulting ranges from strike slip to normal (Table 2). Most of the strike-slip mechanisms have one nodal plane striking north-northwest subparallel to the strike of the aftershock zone. Some of these events could be interpreted as left-lateral motion on southeast striking planes. The cylindrical distributions of many of the small spatial clusters within this zone cannot be used to distinguish between these nodal planes. The normal faulting mechanisms that indicate transtensional faulting have north-northwest or north-northeast striking planes.

In general the aftershocks become shallower to the south. This can be seen in the cross section A-A' that is taken parallel to the aftershock zone (Figure 9b). Both in map view and in the cross section A-A', the Pinto Mountain fault and the Blue Cut faults appear to be aseismic.

The cross sections B-B' through I-I' show how the width of the zone changes from north to south (Figure 9b). Closest to the Landers mainshock (cross section B-B'), on the southernmost extension of the Johnson Valley fault, the aftershocks form a narrow vertical zone. A few kilometers to the south of the mainshock epicenter the aftershock zone becomes wider, as is shown in cross section C-C'. This sudden increase in width of the zone spatially coincides with granitic rocks mapped at the surface [*Bortugno and Spittler,* 1986]. We infer that the increased fault zone width is a feature of the faulting process and not the result of location uncertainty.

Immediately south of the Pinto Mountain fault, the Burnt Mountain and Eureka Peak faults, which had minor

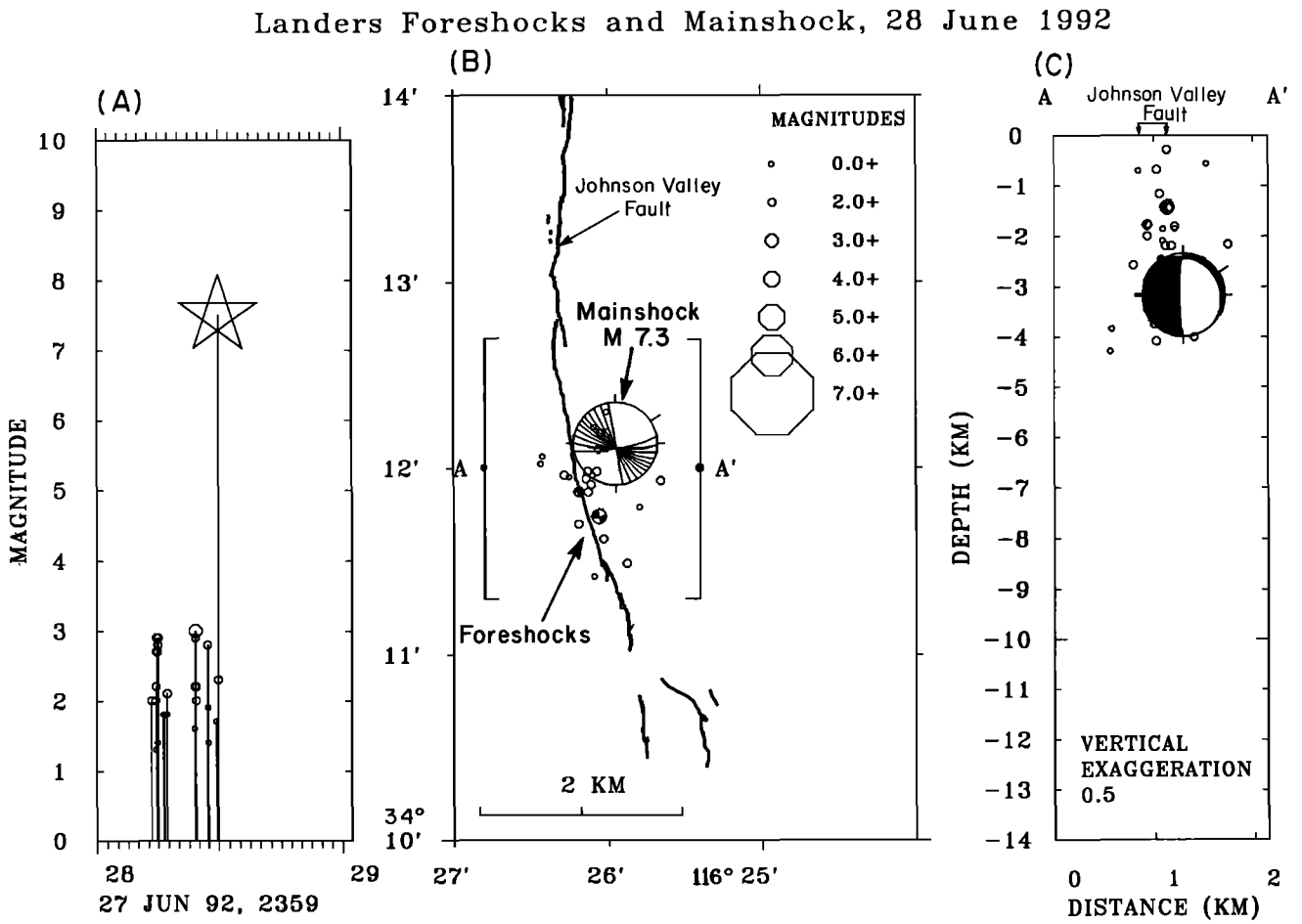

Fig. 8. The Landers mainshock and the foreshocks of the preceding 24 hours. (a) Magnitude versus time for the foreshock-mainshock sequence. (b) Map of the foreshocks showing their location relative to the Johnson Valley fault. The $M7.3$ mainshock and a $M3$ foreshock are represented by their focal mechanisms, the compressional quadrants are shaded with lines. (c) Cross section (vertical exaggeration of 0.5) showing the depth of the foreshocks and mainshock.

surficial offsets of 1 to 20 cm [*Treiman*, 1992], can be seen in the cross sections D-D' and E-E'. *Hough et al.* [1993] propose that these surficial offsets were caused by both delayed triggered slip from the mainshock and from possible slip in the $M5.8$ and $M5.6$ aftershocks that occurred 3 and 4 min after the mainshock, respectively. *Blewitt et al.* [1993] modeled Global Positioning System data and suggested that the Burnt Mountain fault may have had significant slip (more than 1 m) over an 8 km length, and that minor slip occurred on the Eureka Peak fault. Presently, it is not possible to tell from the seismic or geodetic data, if this slip was coseismic during the mainshock or occurred during the first minutes of aftershock activity.

Cross sections F-F' and G-G' show the reactivation of the aftershock zone of the April 23 Joshua Tree earthquake. Farthest to the south the cross sections H-H' and I-I' show the development of a cluster of aftershocks south of the Blue Cut fault that was not well expressed in the aftershocks of the Joshua Tree earthquake (Figure 6). This cluster is bounded on the north side by the Blue Cut fault but none of the aftershocks appear to be on the fault itself.

Because the Landers mainshock ruptured unilaterally to the north [*Kanamori et al.*, 1992; *Wald et al.*, 1992], aftershocks south of the Pinto Mountain fault are, by definition, not occurring on the mainshock fault. The Eureka Peak and Burnt Mountain faults, south of the Pinto Mountain fault, may have been activated only in the two early, big aftershocks or may have experienced a small amount of coseismic slip in the mainshock that cannot be detected in the seismic records. South of these faults (south of 34°N3'), the aftershocks appear to reactivate the Joshua Tree aftershock zone. Although the aftershock activity surged on June 28, the aftershocks in this region died off more quickly than they did farther north, returning to the decay pattern set by the April event.

The unusually large width and complex spatial distribution of the seismic zone suggest that the fault south of the Pinto Mountain fault may be a geologically youthful feature with a small cumulative offset that has not developed into a narrow throughgoing fault. The presence of multiple faults with small cumulative offsets [*Rymer*, 1992] in granitic basement provides numerous potential fault planes and explains the spatially diffuse nature of the

aftershock zone. This is in contrast to the faults north of the Pinto Mountain fault, which have more cumulative slip and are clearly defined.

Landers Mainshock Rupture

The mainshock surface rupture extends 60 km along a north-northwest line, from the epicenter to the northernmost mapped surface offset on the Camp Rock fault (Figure 10). Mapping showed that the rupture occurred on five overlapping, curved fault segments with a cumulative length of 85 km [*Sieh et al.*, 1993]. The rupture initiated approximately 7 km north of the Pinto Mountain fault on a fairly straight stretch of the Johnson Valley fault and propagated north for 18 km. Here it stepped 5 km northward on the newly named Landers fault to the Homestead Valley fault. The rupture continued north for 25 km along the Homestead Valley fault and there stepped to the east, over a 2-km broad shear zone, to the Emerson fault and continued for 32 km. The final 2- to 3-km step was from the Emerson fault to the Camp Rock fault where slip continued for 14 km [*Sieh et al.*, 1993]. The mainshock rupture was modeled from seismic data as two subevents by *Kanamori et al.* [1992]. The first occurred to the south along the Johnson Valley and Landers faults. The second that was twice as large as the first, occurred to the north along the Homestead Valley, Emerson, and Camp Rock faults.

Numerous $M>4.0$ aftershocks occurred near the mainshock rupture zone. One $M5.2$ aftershock that was located near the north end of the rupture on the Johnson Valley fault occurred 43 min after the mainshock. A focal mechanism cannot be determined for this event because it was partially obscured by other aftershocks. A second $M5.2$ aftershock occurred on July 1 at 0740 UT and exhibited oblique thrust motion between the Johnson Valley and the Landers faults. Along the northern half of the rupture several $M>4$, but no $M>5$, aftershocks occurred (Figure 5).

Most of the aftershocks along the mainshock rupture are of $M<4.0$. Near the epicenter of the mainshock the aftershocks form a narrow zone trending N10°W. A dense aftershock cluster 6 km north of the mainshock epicenter is at a small rightstep in the Johnson Valley fault. A large cluster of aftershocks occurred north of the Landers fault, between subparallel segments of the Johnson Valley and Homestead Valley faults. This cluster intersects the Homestead Valley fault where surface slip was less than 1 m [*Sieh et al.*, 1993]. Broadband seismic records [*Kanamori et al.*, 1992] also indicate less slip in this region. A large aftershock cluster between the Emerson and Camp Rock faults coincides with the change in strike at the north end of the Emerson fault and transfer of slip to the Camp Rock fault.

Focal mechanisms of selected representative aftershocks along the mainshock rupture are shown in Figure 10 and listed in Table 2. The aftershocks near the five main fault segments have primarily right-lateral strike-slip mechanisms on north to northwest striking planes. Focal mechanisms exhibiting normal faulting have either north to northwest striking nodal planes consistent with fault normal tension or north to northeast striking planes at the rightsteps in faulting. Along northern end of the Emerson fault there were numerous anomalous focal mechanisms with left-lateral motion on north to north northeast striking planes.

The aftershocks extend from the surface to depths of 15 km. Four cross sections along the mainshock rupture and five orthogonal cross sections are shown in Figure 10. The cross section A-A' spans the Camp Rock fault and shows how the aftershocks became shallower to the north, with no aftershocks along the last 5 km of surface rupture. The cross section B-B' along the Emerson fault shows a concentration of aftershocks in the regions of the fault that overlap with the two adjacent faults. The greatest concentration of aftershocks on the Homestead Valley fault, cross section C-C', is at the slip gap between the two subevents identified first by *Kanamori et al.* [1992]. The Johnson Valley fault, cross section D-D', shows the most activity near the mainshock epicenter and near the rightstep about 6 km north of the mainshock.

The tight spacing of the overlapping fault segments makes it difficult to resolve the corresponding aftershock zones in cross section. Cross section E-E' shows the vertical dip and less than 2 km width of the aftershock zone along the simple section of the Johnson Valley fault. Cross section F-F' spans the Landers fault in the region between the Johnson and Homestead Valley faults. It also includes aseismic segments (segments where no aftershocks occurred) of the two adjacent faults. The region between the Homestead Valley and Emerson faults is a broad shear zone and, in cross section G-G', the aftershocks associated with this shear zone can be seen. Cross section H-H' spans three fault strands, the Emerson and Camp Rock faults to the west and the Calico fault to the east. Cross section I-I' crosses both the Camp Rock and Emerson faults and includes events with focal mechanisms exhibiting left-lateral slip on north striking planes. These anomalous aftershocks are probably in the block east of the Emerson fault. The cross section J-J' reveals both the Camp Rock and Emerson faults.

In general, the spatial distribution of aftershocks along the mainshock rupture is complex and as wide as 10 km (Figure 10). Aftershocks are tightly clustered near the mainshock rupture surface and diffuse away from the rupture surface. The large ($M>3.5$) aftershocks occur primarily at the edges, bottom or top, of the fault strands involved in the mainshock rupture. On several of the fault strands, surface slip was mapped for a few kilometers beyond the ends of the aftershock distributions. This complexity may, in part, be explained by (1) the rupturing of subparallel and overlapping fault segments, (2) the large amount of slip causing an aura of large strains around the rupture, (3) the change in strike of the rupture, starting with northerly strike near the epicenter and gradually rotating with increasing distance to a northwest strike, (4) roughness or small steps along individual fault segments, and (5) variations in slip along the mainshock rupture surface. None of these explanations are mutually exclusive and all may contribute simultaneously to the observed distribution of aftershocks.

Calico and Pisgah Faults

Two trends of aftershocks extend east from the Camp Rock-Emerson faults (Figure 11). A prominent part of these trends are two dense clusters near the Calico and Pisgah faults. The Pisgah cluster is about 2 km wide and

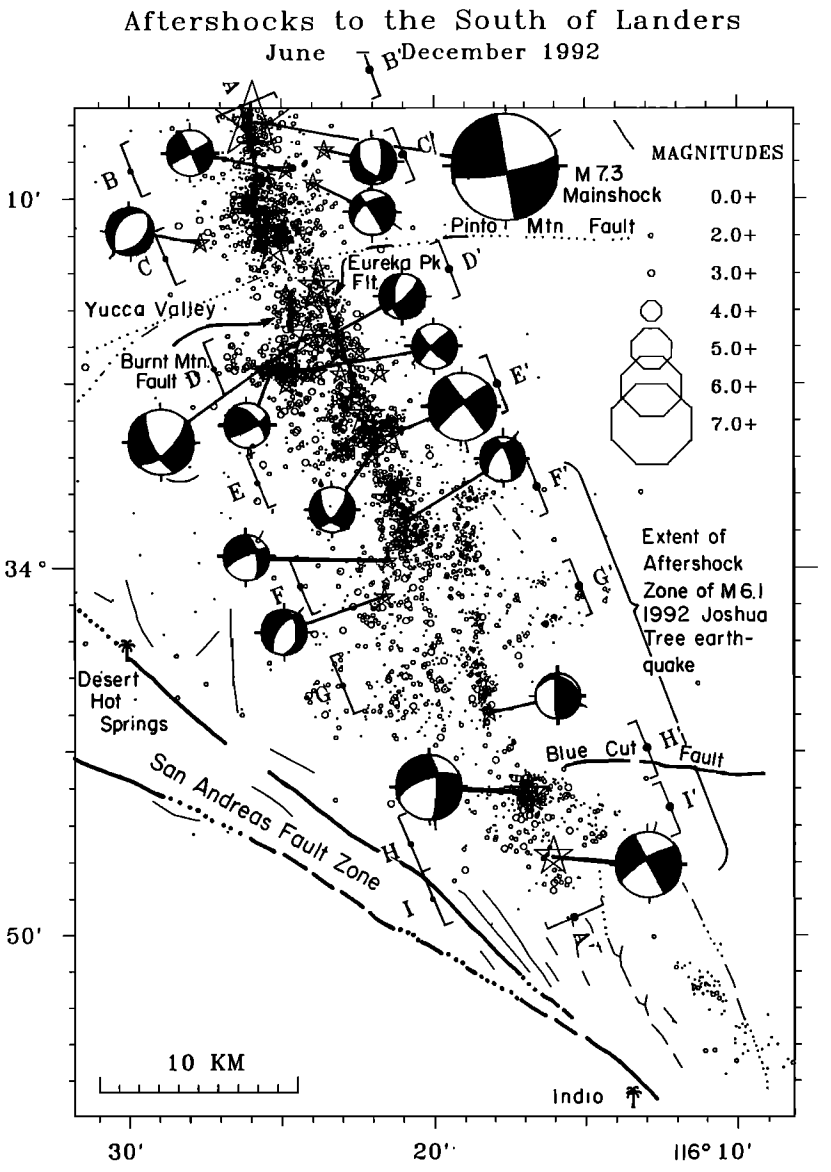

Fig. 9a. Aftershocks south of the M_W7.3 Landers mainshock epicenter. Map showing major faults (dotted where inferred) and locations of aftershocks from June 28 to December 31, 1992. Lower-hemisphere first-motion focal mechanisms of typical events are also shown. The spatial extent of the 1992 Joshua Tree aftershock zone is also indicated. End points of cross sections A-I in Figure 9b are also shown. Earthquakes of $M \geq 4.0$ are shown by stars.

10 km long. It began with a series of small aftershocks and culminated with one of the largest aftershocks of the sequence, a M_L5.4, which occurred on July 5, 1992, at 2118 UT. The focal mechanism of this event exhibited oblique right lateral thrust motion in the plane striking north-northwest, parallel to the trend of seismicity (Table 2). The cluster located on the west side of the Calico fault had mostly pure strike-slip mechanisms. The aftershocks in the two east trends are distributed vertically extending from the surface down to depths of 8 to 12 km as shown in cross sections A-A' and B-B' (Figure 11). The Calico cluster is confined to depths of 4 to 12 km and the Pisgah cluster extends from the surface to a depth of 8 km.

The eastward trend of the aftershocks to the Calico fault corresponds to small surface offsets mapped on unnamed northeast striking faults [*Hart et al.*, 1993]. The two east trends could reflect an unsuccessful jump of the rupture front to the Calico fault or the activation of left-lateral cross faults. Alternatively, these aftershocks and mapped surface offsets on north striking faults [*Sieh et al.*, 1993] may be indicators of off-fault strains caused by the change in strike from N10°W to N45°W along the mainshock rupture surface. This change in strike could cause the block on the east side to fracture and possibly rotate along right-lateral north striking faults and left-lateral east striking faults. The spatial association of these clusters with existing major fault zones suggest that these may be weak zones or have high applied shear stress.

Following the Landers mainshock 9 cm of right-lateral triggered slip [*Hart et al.*, 1993], but no aftershocks,

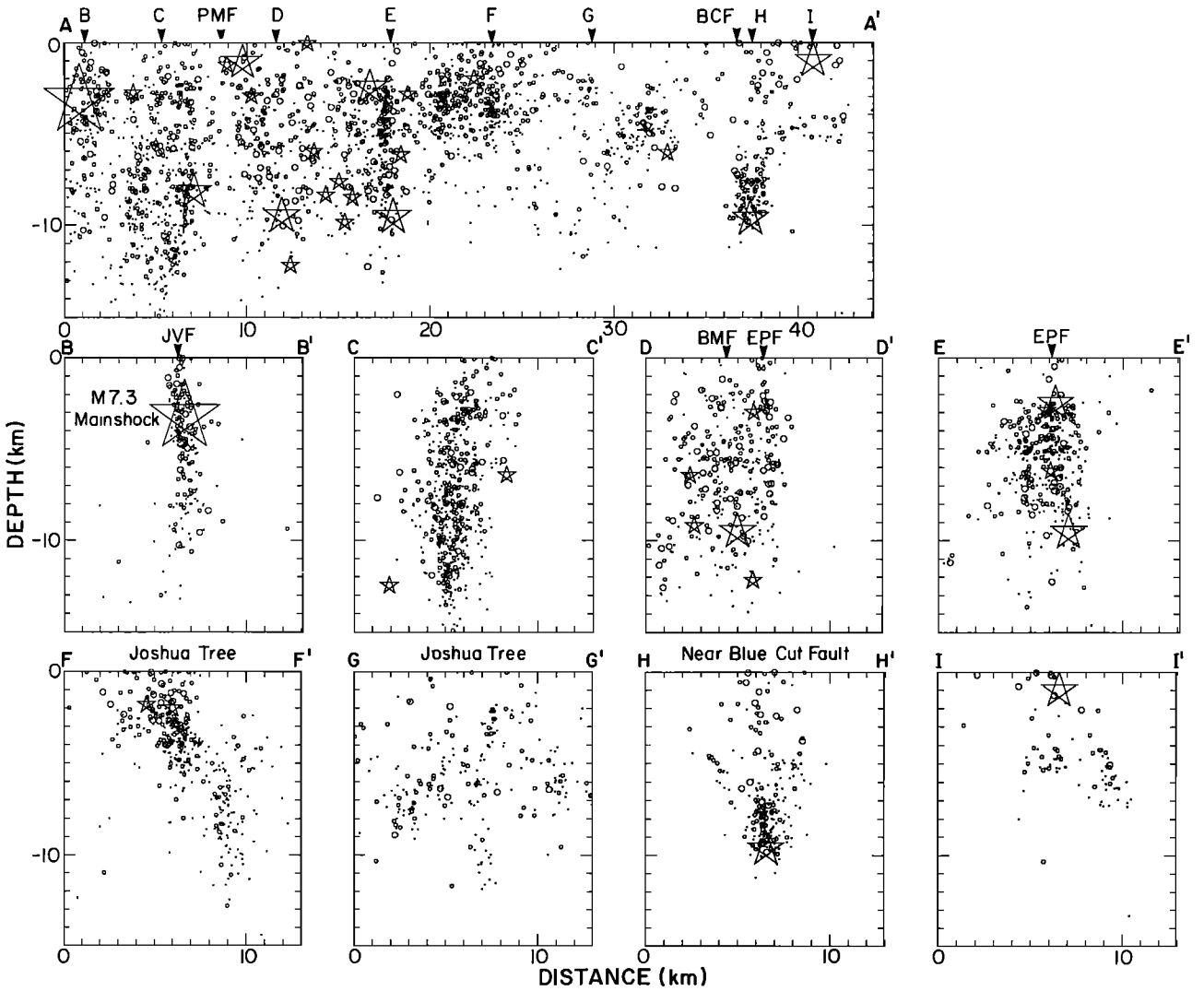

Fig.9b. Cross sections, as indicated in Figure 9a, parallel to the long axis of the distribution (A-A') and orthogonal to the distribution, B through I. PMF, Pinto Mountain fault; BCF, Blue Cut fault; JVF, Johnson Valley fault; BMF, Burnt Mountain fault; and EPF, Eureka Peak fault. Earthquakes of $M \geq 4.0$ are shown by stars.

occurred along the Galway Lake fault even though it was within a few kilometers of the Emerson fault. In comparison, an earthquake sequence with a $M_L 5.2$ mainshock occurred in 1975 at only 2 km depth [*Lindh et al.*, 1978] and produced right-lateral surface offsets on this fault of 0.2 to 1.5 cm in 1975 [*Hill and Beeby*, 1977]. The two east trends are located just to the north of the 1975 Galway Lake aftershock zone and thus are not a reactivation of the 1975 aftershock zone.

Barstow Sequence

The Barstow sequence of aftershocks, separated from the main group by 30 to 40 km, is located 10 to 20 km to the north of the City of Barstow (Figures 4 and 12). It began 6 to 8 hours following the Landers mainshock and the largest event of $M4.8$ occurred on August 5, 1992. The cluster is approximately 20 km long, 2 to 3 km wide, and strikes north-northwest (Figure 12). The narrow width, about 2 km, of the Barstow sequence is a good indicator of the available location accuracy in the region. In addition, the narrow width indicates that the Barstow sequence occurred on a single fault, unlike the Landers mainshock, which occurred on multiple subparallel fault strands. The Barstow sequence does not coincide with any of the many surficial faults in the region. Instead, it intersects, at an angle of 10° to 20°, the Blackwater-Calico faults, the longest fault system in the central Mojave, which strikes north-northwest for 200 km, from the Pinto Mountain fault to the Garlock fault [*Dokka and Travis*, 1990b]. Unlike previous moderate earthquakes in the Mojave Desert (e.g., the 1979 Homestead Valley earthquake), the Barstow sequence shows a tight linear distribution and extends deeper to about 10 km depth.

Adjacent to the Barstow sequence other smaller clusters of seismicity can be identified in Figure 12. East of Barstow, one of these clusters occurred where the Calico fault exhibits a more westerly strike. North of the Calico fault cluster, scattered aftershocks occurred adjacent to the Coyote Lake fault, near the eastern boundary of Superior Valley. Northwest of the Barstow cluster, three $M4$ events occurred near the Harper fault (Figure 12). All of

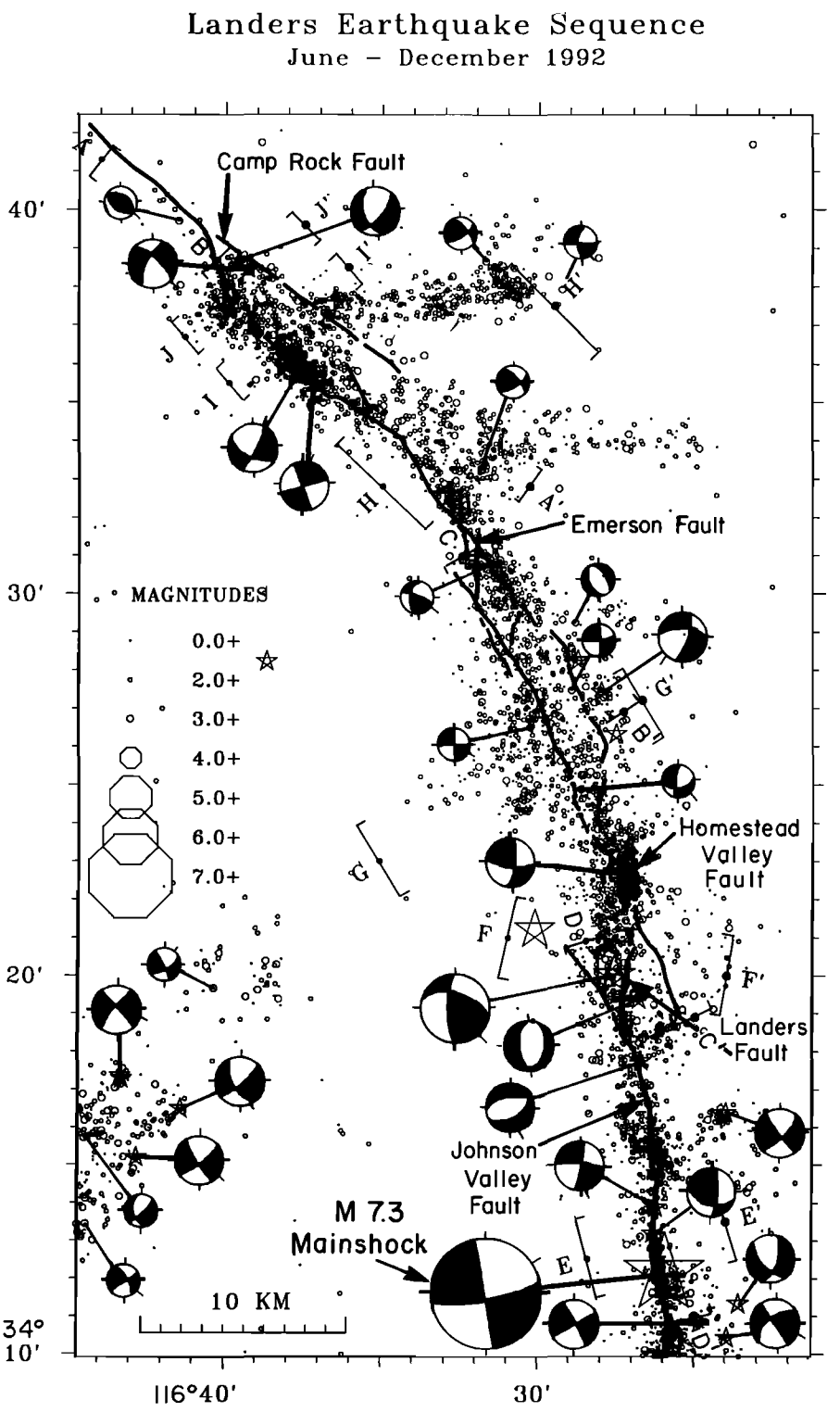

Fig. 10a. Map showing aftershocks along the Landers mainshock rupture and locations of aftershocks from June 28 to December 31, 1992. The heavy line indicates the surface rupture [Sieh, 1993]. Lower-hemisphere first-motion focal mechanisms of typical events are also shown. End points of cross sections A-J in Figure 10b are also shown. Earthquakes of $M \geq 4.0$ are shown by stars.

these clusters occurred close to or within mapped surficial late Quaternary fault zones.

Most of the focal mechanisms of the events in the Barstow sequence show right-lateral strike-slip motion on north-northwest to north striking planes. The strike-slip style of faulting is consistent with the orientation of late Quaternary surficial faulting in the Mojave Desert summarized by *Dokka and Travis* [1990a]. In a few cases the focal mechanisms have some normal component, probably associated with bends or en echelon offsets in the strike-slip faults.

The cross sections in Figure 12 indicate that, in general,

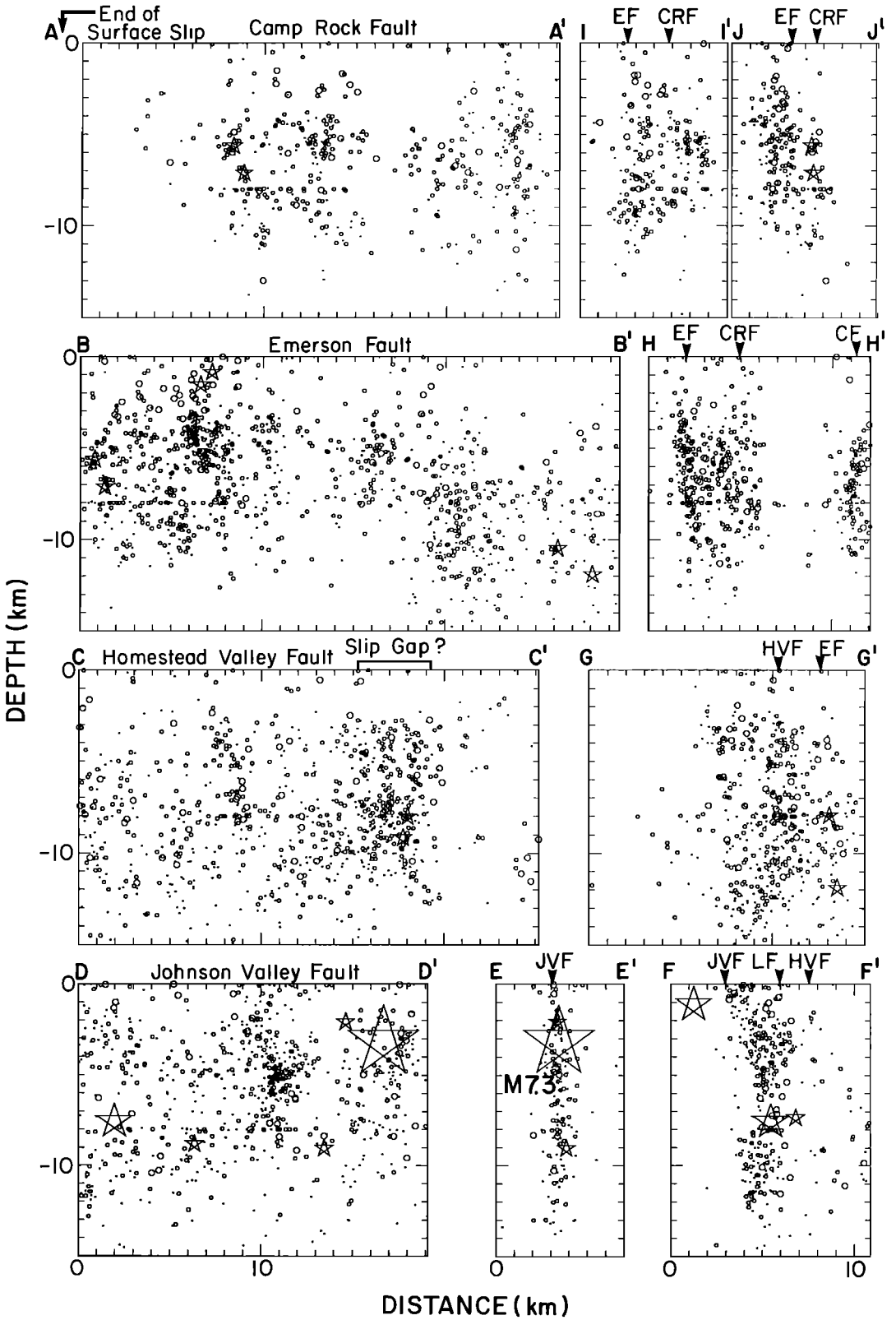

Fig. 10b. Cross sections, as indicated in Figure 10a, parallel to the long axis of the distribution, A through D, and orthogonal to the distribution, E through J. EF, Emerson fault; CRF, Camp Rock fault; HVF, Homestead Valley fault; JVF, Johnson Valley fault; and LF, Landers fault. Earthquakes of $M \geq 4.0$ are shown by stars. The region marked "slip gap?" is the region between sub-events identified by Kanamori *et al.* [1992] as experiencing minimal slip in the mainshock.

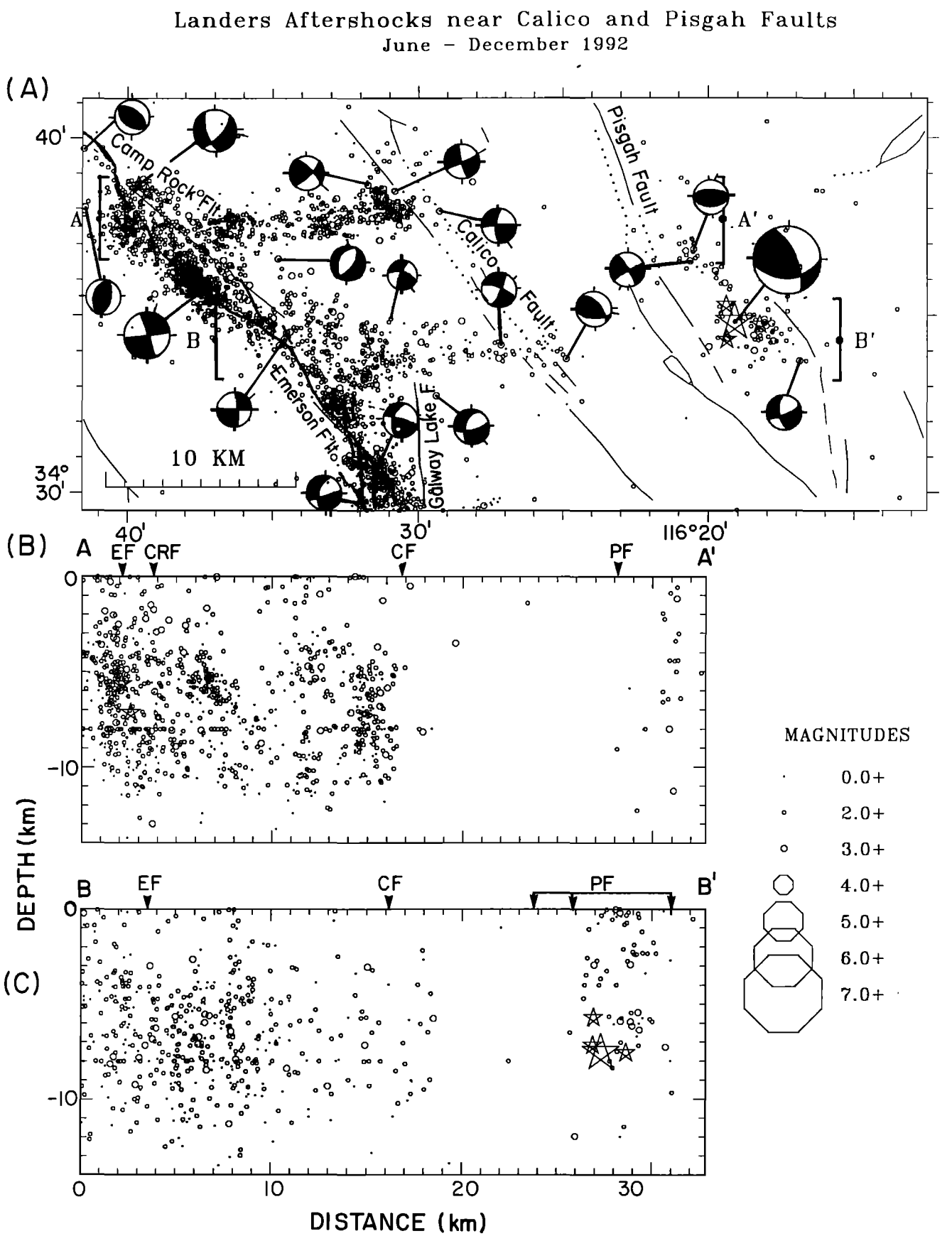

Fig. 11. Detail of Figure 10. Aftershocks along the mainshock rupture, Emerson and Camp Rock faults, and near the Calico and Pisgah faults. (a) Map showing major faults (dotted where inferred) and locations of aftershocks from June 28 to December 31, 1992. Lower-hemisphere, first-motion, focal mechanisms of typical events are also shown. (b) East-west cross section showing depth distribution of the Calico cluster. EF, Emerson fault; CRF, Camp Rock fault; CF, Calico fault; PF, Pisgah fault. (c) East-west cross section across the Pisgah fault cluster. Earthquakes of $M \geq 4.0$ are shown by stars.

the earthquake focal depths of the Barstow region are shallower than the focal depths along the Landers mainshock rupture. The three $M>4$ events in cross section A-A' are located near the Harper fault. In cross section B-B', along strike of the main Barstow cluster, the depth distribution is fairly uniform from 0 to 10 km. Cross section C-C' along the east side of Superior Valley shows that those events are shallow, above 5 km. The cross section D-D', parallel to the strike of the Calico fault, shows the vertical cluster at the turn in the Calico fault toward the west. These events are as deep as the aftershocks on the mainshock faults, down to 15 km. The Barstow cluster extends to 10 km, and the scattered activity near the Coyote Lake fault extends to 7 km depth as shown in cross sections E-E' and F-F'. Overall, the distributions of the aftershocks are consistent with strike-slip faulting on vertical or almost vertical faults.

Many faults of the northern and southern Mojave block converge in the Barstow region [*Dokka and Travis*, 1990a], producing complex late Quaternary structures. Several late Quaternary anticlines and synclines have also been mapped in the Barstow area [*Bartley et al.*, 1990]. The trend of the Barstow cluster suggests that none of the major surficial faults are, at present, favorably oriented for failure. Similarly, the absence of thrust focal mechanisms and dipping or subhorizontal distributions of seismicity suggests that the compressive tectonic structures are likewise seismically inactive.

Big Bear Sequence

The Big Bear sequence was 30 to 40 km west of the main fault system of the Landers earthquake. It began almost 3 hours after the Landers mainshock with an $M5.3$ event at 1443 UT June 28, 1992 (Figure 13). Twenty-two minutes later, at 1505 UT, the largest Landers aftershock, the $M6.2$ Big Bear earthquake, occurred at 34°09.9'N, 116°49.3'W. An $M4.3$ foreshock preceded this earthquake by 40 s. This makes the location of the mainshock uncertain and the first-motion focal mechanism unconstrained. In general, many foreshocks are within 1 km of the mainshock [*Jones*, 1984], and they often have focal mechanisms very similar to their mainshock. Also, an independent study of the S waveforms recorded by TERRAscope [*Thio and Kanamori*, 1992] obtained a focal mechanism for the Big Bear earthquake very similar to that of the foreshock. We therefore assign the location and focal mechanism of the foreshock to the Big Bear earthquake. The assigned hypocenter puts the Big Bear earthquake at the southwestern end of the densest part of the northeast striking aftershocks. The assigned focal mechanism of the Big Bear earthquake has one nodal plane striking N55°E and dipping 85° with a rake of -10°. Thus the $M6.2$ Big Bear earthquake probably was caused by left-lateral motion on a northeast striking fault rupturing unilaterally to the northeast for a distance of approximately 15 km. Its foreshock and aftershocks have a depth range of 0 to 13 km.

The Big Bear earthquakes have several noteworthy features. First, they approach the San Andreas fault zone near Yucaipa but the spatial distribution and focal mechanisms do not suggest motion on any of the many fault strands within the San Andreas fault zone. Second, a minor, northeast striking trend of aftershocks is 4 to 8 km northwest of the Big Bear earthquake trend, suggesting that subparallel faults were activated. Third, in addition to these two faults, a diffuse group of earthquakes formed 15 to 20 km to the north of the Big Bear earthquake, just west of the intersection of the Helendale and NFFZ. Within this group several dense spatial clusters of seismicity are observed, including the aftershocks associated with the $M \geq 5$ aftershocks in November and December 1992. The activity south of the main Big Bear trend is typical of the rate and location of background seismicity. Fourth, the absence of aftershocks between the Lenwood fault to the Landers mainshock fault is considered to be real.

Representative focal mechanisms for the bigger aftershocks in this sequence are shown in Figure 13. Most of the focal mechanisms are consistent with left-lateral strike-slip motion on north-northeast to northeast striking faults. Two events showed thrust motion. One event, on August 17 near the Big Bear earthquake, was thrust on a northeast striking plane, inconsistent with the strike of any Quaternary thrust fault in the region. The other, on December 4, was in the northern group and appears to be on the south dipping NFFZ at shallow depths (about 3 km). The NFFZ was not active until December. The overall lack of thrust faulting events suggests that the major thrust faults within the San Bernardino Mountains are not participating in the tectonic deformation of the region caused by the Landers sequence. This is also consistent with the dominance of strike-slip focal mechanisms in this region reported previously by *Webb and Kanamori* [1985].

The depth distribution of the Big Bear seismicity is illustrated in Figure 13. The cross sections A-A' and B-B' are parallel to the Big Bear aftershock trend. The A-A' cross section extends from the San Andreas fault along the strike of the $M6.2$ event nodal plane to just southeast of the Homestead Valley fault. The cross section B-B' extends from the San Jacinto fault in the southwest to the Lenwood fault in the northeast. The Lenwood fault bounds the Big Bear sequence on the northeast side. Cross section A-A' shows how the seismicity shallows both to the northeast and to the southwest. The aftershocks are deepest at 13 to 15 km near the focus of the Big Bear earthquake. Cross section B-B' shows a cluster of earthquakes near the San Andreas fault at Yucaipa and other vertical clusters and the arcuate maximum depth of faulting, extending from the Mill Creek fault to the Helendale fault. The seismicity near the Crafton Hills fault may be part of the regular background activity. The Yucaipa cluster is shown in more detail in the fault-parallel cross section C-C'. The focal mechanism of the largest Yucaipa event has a plane parallel to the San Andreas fault but the cross sections B-B' and C-C' do not reveal a clear spatial relationship to any of the known strands of the fault.

The three northwest-southeast trending cross sections, D-D', E-E', and F-F', show several features. Foremost is the steeply dipping distribution of the aftershocks of the Big Bear earthquake. Most isolated dense clusters of aftershocks appear to have vertical distributions. The cross section D-D' includes most of the seismicity southwest of the mainshock. The cross section E-E' includes activity in the mainshock area and on either side, showing the vertical distribution of seismicity in these individual seismicity clusters. The cross section F-F' includes the north end of

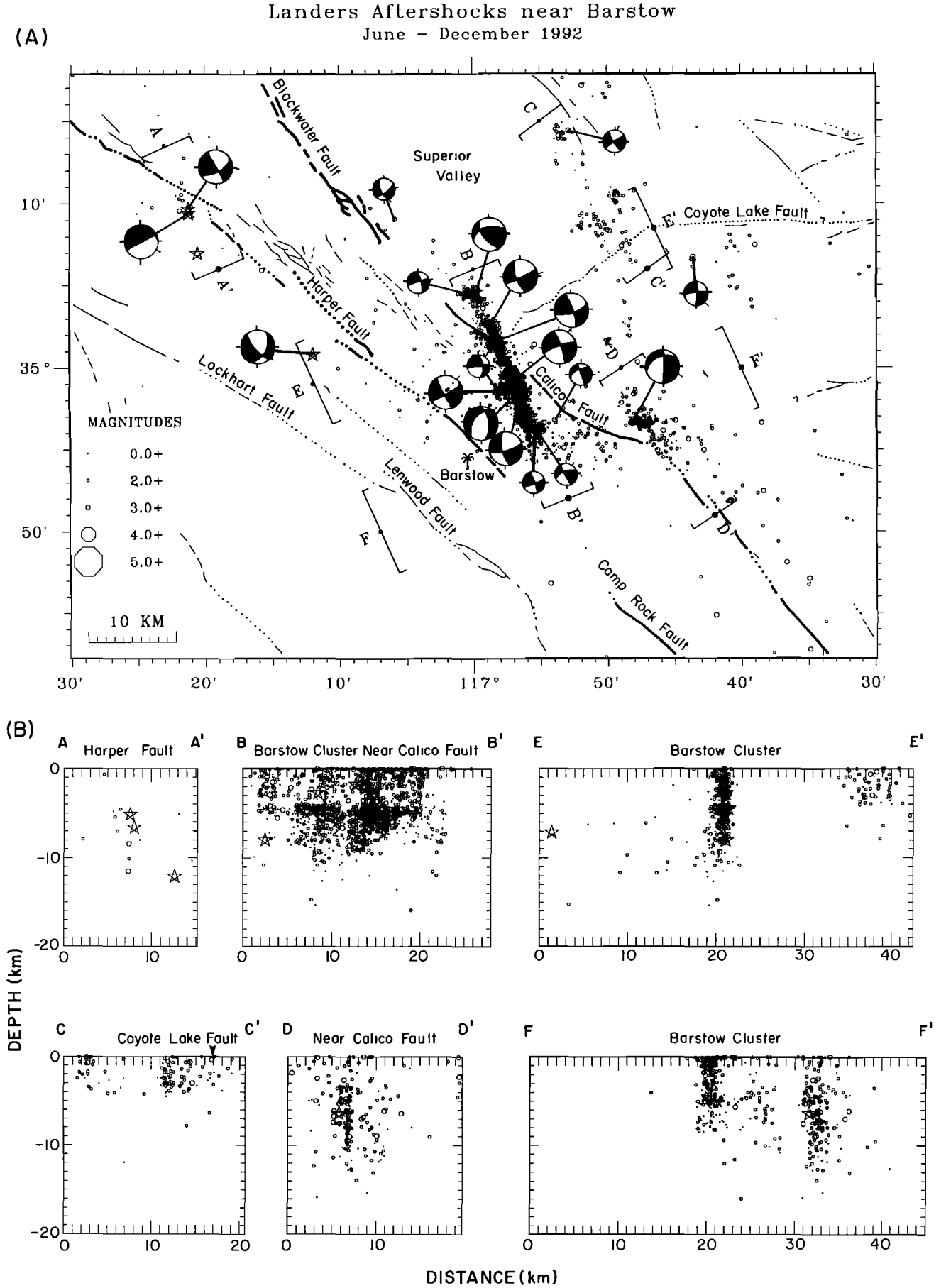

Fig. 12. Aftershocks near Barstow. (a) Map showing major faults (dotted where inferred) and locations of aftershocks from June 28 to December 31, 1992. Lower-hemisphere, first-motion, focal mechanisms of typical events are also shown. (b) Cross sections showing the depth distribution of aftershocks. Earthquakes of $M \geq 4.0$ are shown by stars.

the $M6.2$ rupture zone and the aftershocks that occurred in late November and early December. Respective focal mechanisms suggest that the November 27 ($M5.3$) event occurred on a northeast striking left-lateral fault while the December 4 ($M5.1$) shock occurred near the NFFZ. This late activity and the earlier Big Bear earthquakes suggest an apparent step in the crustal structure at depth, reflected by the shallow aftershocks to the north and the deep aftershock to the south, as can be seen in cross section F-F'.

The map in Figure 13 includes the aftershock zone of the 1986 $M_W5.9$ North Palm Springs earthquake [*Jones et al.*, 1986]. Almost no seismicity occurred in this zone indicating that it did not participate in the Big Bear deformation.

The Big Bear sequence is confined within the San Bernardino Mountains block, bounded on the north by the NFFZ [*Meisling and Weldon*, 1989] and the south by the north branch of the San Andreas fault zone and the Mill Creek fault [*Matti et al.*, 1992]. The overall shallowing of the aftershocks to the north as well as to the south indicates that the south and north bounding faults play a role in creating spatial boundaries for the deformation. The fracturing of the San Bernardino Mountains block along northeast striking strike-slip faults suggest that most of the late Quaternary thrust faults in the region were not activated by the Landers sequence. The movement of blocks around the "big bend" of the San Andreas fault appears to be accomplished by mostly lateral movement of crustal blocks at the present time as opposed to block shortening or extension.

Temporal Development

The aftershocks decay as predicted by Omori's Law [e.g., *Utsu*, 1961] with an average p value of 0.97 ± 0.04. Seismicity in all of the regions is decaying at approximately the same rate with the exception of the region of the Joshua Tree mainshock. If these aftershocks are assumed to be decaying from a mainshock on June 28, the p value is 1.20. However, the temporal distribution of the aftershocks south of latitude 34°03'N is better fit by assuming a mainshock on April 23 (the Joshua Tree earthquake). The p values determined for April 23 through June 27 and for April 23 through December 31 in this region are in both cases 0.72. We therefore consider events in this region to be aftershocks of the Joshua Tree earthquake.

Landers rupture zone. The aftershock zone developed rapidly and most of the aftershock zone was defined in the first 3 days. In July, however, the Pisgah fault cluster emerged as a new cluster of activity. The aftershock zone extending 40 km to the south of the $M7.3$ epicenter showed a high rate of activity in June and July and then in the subsequent months returned to the decay rate expected from the Joshua Tree earthquake. The aftershocks along the mainshock rupture decayed more slowly.

Decrease in width of the aftershock zone and the frequency of large $M>4$ aftershocks in October, November, and December reflects the expected rate of decay. If the present rate continues, seismicity in this region will stay above background levels for about 8 years.

Barstow region. The Barstow sequence started slowly in June 28 through 30 and was limited to an area south of the Calico fault. In July it expanded to the north-northwest across the Calico fault and several new clusters, located to the east of the main cluster, flared up for short time periods. One of these clusters suggests a 5-km-long north-northwestward extension of the Calico fault. In August through November the Barstow cluster had aftershocks at a steady rate but did not show an increase in its spatial dimensions.

Big Bear region. The spatial extent of the Big Bear sequence changed most with the timing of the three sequences. Many $M>4$ aftershocks defined the Big Bear earthquake rupture zone even within the first day. The Yucaipa cluster near the San Andreas fault produced two $M4$ aftershocks in June. In July, a large cluster developed just north of the mainshock epicenter and the aftershocks extended to fill in the gap between the Yucaipa cluster and the main zone. The earthquake activity southeast of the Big Bear trend and within the San Andreas fault zone varies little from June to November, indicative of the background activity in this region.

In late November and early December the aftershock activity increased over a 2 week time period north of Big Bear, near the NFFZ, but still within the aftershock zone as it was defined by early July. Overall, the aftershock activity was slightly higher during November than in October.

In summary, the outer limits of the Landers aftershock sequence were established within a few days and later developments in almost all cases occurred within these limits. This suggests that the wide spatial distribution of Landers aftershocks is indeed related to the occurrence of the mainshock.

DISCUSSION

Precursors?

The 1992 Landers sequence occurred along the western edge of the ECSZ where two $M5+$ earthquakes had occurred in 1975 and 1979. In retrospect, some aspects of the 1975 $M_L5.0$ Galway Lake and the 1979 $M_L5.3$ Homestead Valley sequences suggest that much of the ECSZ was close to failure. Both earthquakes produced surficial offsets on faults of late Quaternary age with strikes inconsistent with their aftershock distributions. Both aftershock sequences were scattered over a relatively broad region, greater than the lengths of the mainshock rupture on many small faults and all at shallow depths, above 6 km. The wide spatial scatter of aftershocks suggests that the whole region was close to failure.

The maximum depth of faulting for the Landers aftershocks ranged down to 12 to 15 km, significantly deeper than in the previous sequences. The greater focal depth distribution suggests that the 1992 Landers earthquake ruptured through the whole brittle crust while the previous $M5+$ mainshocks in the region only released stress in the upper part of the brittle crust.

The Galway Lake, Homestead Valley, and Landers earthquakes were all preceded by foreshocks [*Lindh et al.*, 1978; *Hutton et al.*, 1980; *Jones*, 1984]. The Homestead Valley sequence had a principal foreshock one magnitude unit bigger than the other foreshocks, less than 1 hour before the mainshock, while the Galway Lake and Landers foreshocks were more like earthquake swarms with many small events. The Galway Lake sequence began 12 weeks before the mainshock with very small events and then had

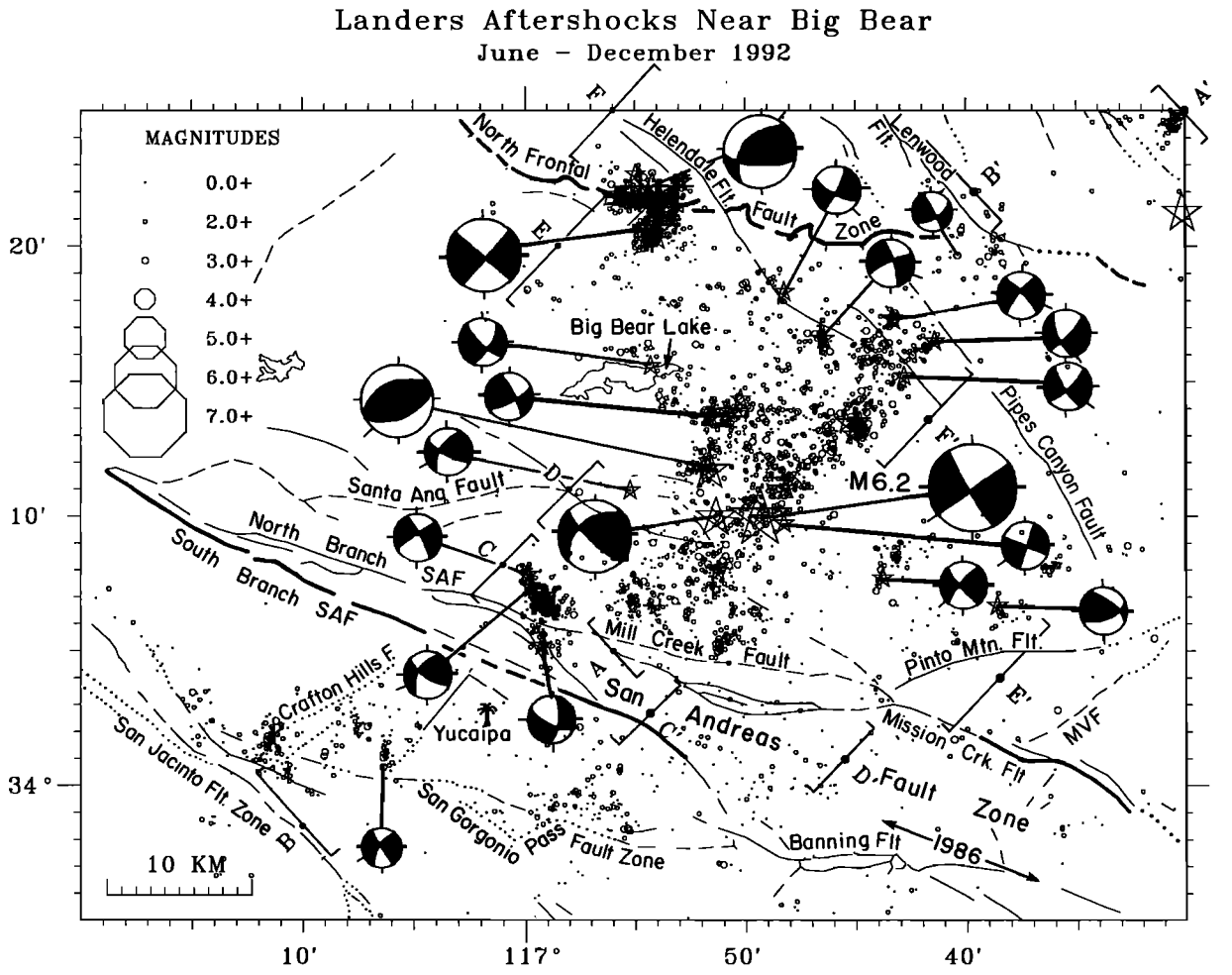

Fig. 13a. Aftershocks in the Big Bear region. Map showing major faults (dotted where inferred) and locations of aftershock from June 28 to December 31, 1992. Lower-hemisphere, first-motion, focal mechanisms of typical events are also shown. The 1986 $M5.9$ North Palm Springs aftershock zone is indicated with a line and the year 1986. End points of cross sections A-F in Figure 13b are also shown. Earthquakes of $M \geq 4.0$ are shown by stars.

several $M3$ events in the last day. The Landers sequence began 12 hours before the mainshock with at least 25 small events. In all three cases, the foreshocks were confined to a small region (1 to 2 km) that became the epicenter of the mainshock at shallow depths. No feature of these foreshocks obviously distinguished them from background seismicity before the mainshock occurred, although *Mori and Jones* [1992] have shown that the Landers foreshocks were more tightly clustered in space than other Joshua Tree aftershocks.

Abercrombie et al. [1992] have shown that the mainshock itself was part of an accelerating process and started off as an $M4$-$M5$ event that within 3 s began growing into a larger $M7.3$ earthquake. Together with the similarity in the foreshock sequences and the shallow hypocenter of the mainshock, this suggests the Landers earthquake began as an earthquake very similar to the 1979 Homestead Valley earthquake that then triggered a larger, deeper earthquake. It also shows that moderate and large earthquakes in the ECSZ occur at different depths in the crust and that the background seismicity in this case cannot be used to predict the maximum depth of large events.

Style of Faulting

At least 20 late Quaternary faults were involved in the deformation of the Landers sequence. Some of the faults were mapped as active late Quaternary faults prior to the earthquake sequence [*Bortugno and Spittler*, 1986]. Others cannot be observed at the surface and are known only because they caused aftershocks. The spatially heterogeneous nature of the aftershock distribution is consistent with the complex fault jumping exhibited by the surface rupture [*Sieh et al.*, 1993]. Clusters of aftershocks occur near both ends of the rupture and in areas where the mainshock rupture steps over from one fault segment to the next.

Frequent swarms of small earthquakes have been recorded over the last two decades south of the Pinto Mountain fault in the general vicinity of the 1992 $M6.1$ Joshua Tree earthquake. In general, this region is characterized by a lack of surficial, mapped faults with significant cumulative offsets [*Rymer*, 1992]. The Joshua Tree aftershocks occurred on many small faults, causing the aftershock zone to be about twice as wide as it was farther north on the Johnson Valley fault. The presence of this aftershock zone

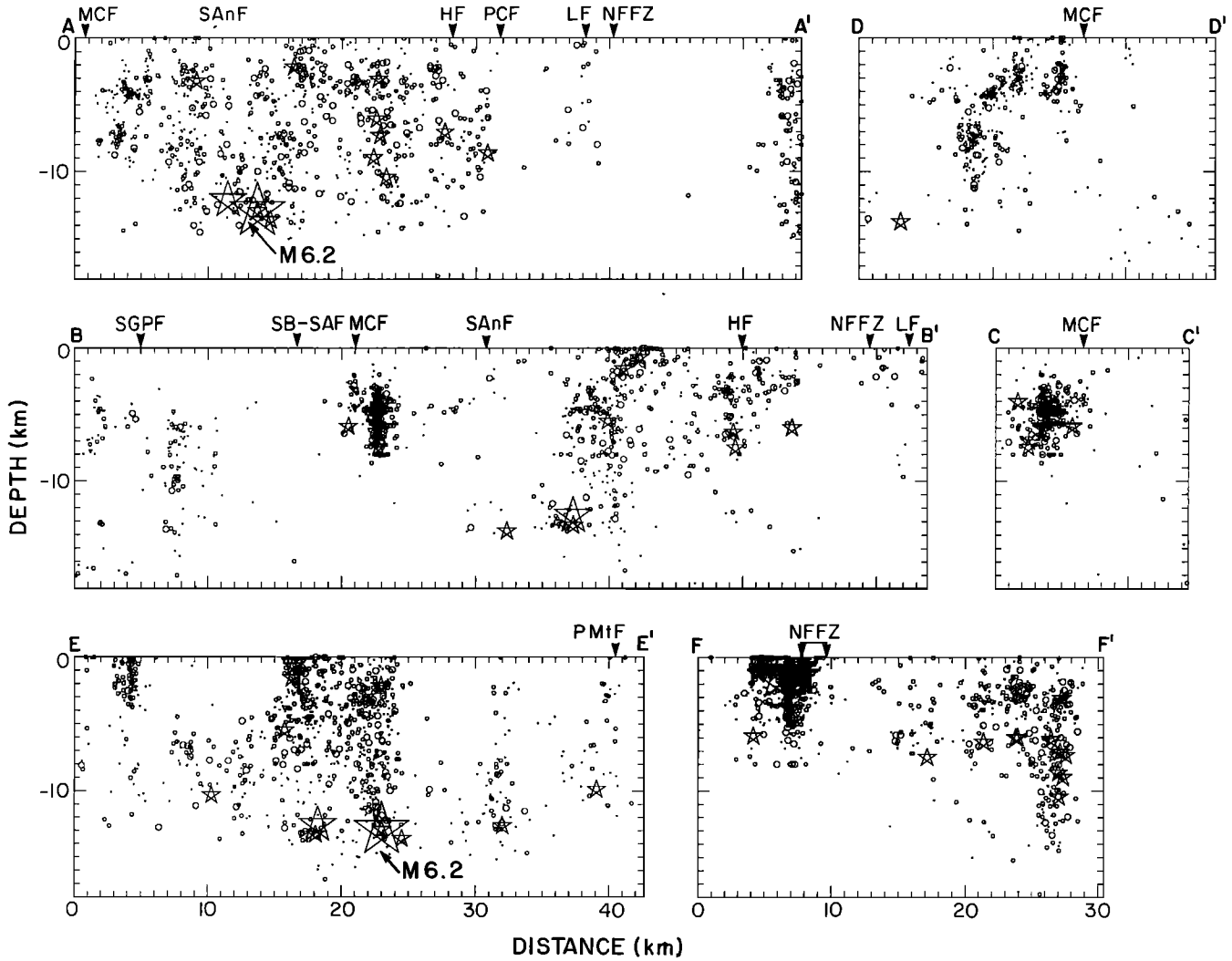

Fig. 13b. Cross sections, as indicated in Figure 13a, showing the depth distribution of aftershocks. SAnF, Santa Ana fault; HF, Helendale fault; PCF, Pipes Canyon fault; LF, Lenwood fault; NFFZ, North Frontal fault zone; MCF, Mill Creek fault; SGPF, San Gregonio fault; SB-SAF, south branch of the San Andreas fault; and PmtF, Pinto Mountain fault. Earthquakes of $M \geq 4.0$ are shown by stars.

and the geologic observation from *Dokka and Travis* [1990a] that Mojave faults to the south of Barstow in general have higher slip rates than faults to the north suggest future large earthquakes may occur along the seismic zone south of Landers. Such large events would be links in a chain of events that transfer slip from the San Andreas fault zone into the ECSZ.

The 15 to 25 km of activity just south of the mainshock epicenter could be an end effect of the mainshock dislocation (Figure 9). The events farther south appear to be Joshua Tree aftershocks that briefly surged after the Landers earthquake, much like a secondary aftershock sequence.

The 1992 Joshua Tree preshock sequence showed right-lateral strike-slip faulting on a N10°W striking plane, consistent with the numerous north striking faults mapped east of the San Andreas fault in the region [*Rymer*, 1992]. The predominance of strike-slip faulting in the Little San Bernardino Mountains was also seen in background seismicity of the region [*Williams et al.*, 1990]. The dominance of strike-slip deformation was expected in the Mojave region as part of the movement of crustal blocks suggested from geological data by *Dokka and Travis* [1990a]. The Landers earthquake itself, however, did not respect the previously identified block boundaries and ruptured across many different fault segments. Along the sequence of fault ruptures the deformation is nearly all strike slip with a few dip-slip mechanisms. The occurrence of two major strike-slip faulting aftershock clusters, both to the south and to the north of the Landers rupture could be interpreted as a result of end effects, or as additional strain release needed to complete the regional strain release.

The Barstow cluster has some similarities with the 1979 Homestead Valley sequence. It did not occur on a major mapped fault in the region but rather defined a new trend crossing the Calico-Blackwater fault system. Its location, however, does not preclude future activity on the major late Quaternary faults in the Barstow region, just as the occurrence of the Homestead Valley sequence on an unknown north-striking fault did not preclude the Landers

event. The long lengths of the nearby surficial faults suggest that these faults can cause earthquakes of similar magnitude as the M_W7.3 Landers earthquake. Hence their earthquake potential should be included in future seismic hazards assessments for the region.

The Big Bear cluster which is spatially separated from the main aftershock trend, may have resulted from the complex redistribution of stresses caused by the mainshock [*Stein et al.*, 1992; *Harris and Simpson*, 1992]. It also exhibited mostly strike-slip deformation, left-lateral slip on northeast striking planes. This is unexpected because northeast striking faults have not been mapped in the region, and the San Bernardino Mountains are bound by a major thrust fault on the north side, the NFFZ, and smaller thrust faults on the south side, such as the Santa Ana, San Gorgonio, and Banning faults. The lack of thrust faulting during this sequence suggests that slip partitioning may occur in this region and the Landers stress field is activating only the strike-slip faults.

The dominance of strike-slip faulting suggests that crustal block translation or rotation is an important part of the deformation adjacent to the plate boundary [*Weldon and Humphreys*, 1986]. A determination of which fault segments form the important boundary faults needs to be included in future seismic hazard analysis. The region between the Big Bear earthquake and the Landers rupture moved to the north-northeast away from the San Andreas fault during this sequence. Because the slip in the Landers earthquake is at least twice the slip in the Big Bear earthquake this crustal block may have rotated counterclockwise at the same time.

Regional Tectonics

The 1992 Landers sequence reflects the complexity of present-day tectonics in southern California. Although the Landers sequence occurred outside the San Andreas fault zone, the main plate boundary in southern California, it is related directly to ongoing deformation along that boundary. It occurred where the San Andreas fault changes strike from N35°W to N65-75°W. In this region the trend of the relative plate motion vector is N36±2°W [*DeMets et al.*, 1990]. The strike of the Landers fault zone, N10°-45°W, and the right-lateral sense of motion suggest that the Landers fault zone contributes to the plate motion [*Savage et al.*, 1990].

The 1992 Landers earthquake provides a mechanism for transferring slip along the Eastern California Shear Zone. Eventually, this slip is transferred along faults crossing the Mojave Desert into the southern Basin and Range [*Dokka and Travis*, 1990a]. The slip appears to be transferred from the San Andreas fault zone, across the Little San Bernardino Mountains, to the Landers fault zone by regional shear (slip on multiple parallel right-lateral faults striking north to northwest) of the western part of the range as opposed to transferring the slip on one throughgoing fault.

CONCLUSIONS

The Landers earthquake sequence wrote a new chapter in the seismotectonics of southern California by imaging the complex fault structures in the Eastern California Shear Zone and the San Bernardino Mountains. The large volume of new data have provided new observations about spatial and temporal characteristics of such large sequences. We have found that the characteristics of the faults as mapped at the surface are well matched by the seismicity. South of the Pinto Mountain fault and in the San Bernardino Mountains, the faults are young and not well developed at the surface. The seismicity in these regions is energetic and diffuse. Major faults bound these regions, such as the San Andreas, Pinto Mountain and Blue Cut faults, but none of these were activated in the sequence. In the northern parts of the aftershocks zone, the faults are better defined with larger cumulative offsets. This region recorded significantly fewer large aftershocks and the aftershocks zones are narrower.

Many of the earthquake sequences of the last 20 years were reactivated by the Landers earthquake. The 1975 Galway Lakes and 1979 Homestead Valley earthquake zones are adjacent to the Landers zone. Although rupture from the Landers mainshock did not propagate into the rupture zone of the April 23, 1992, Joshua Tree earthquake, aftershocks to that earthquake surged with the occurrence of the Landers earthquake. The Landers aftershocks occurred at greater depths than those to the 1975 and 1979 mainshocks, but the foreshocks and initial depth of the Landers mainshock were similarly shallow. Together with waveform observations, this suggests that the Landers earthquake began as a shallow moderate event that triggered a deeper, larger earthquake within a few seconds.

The dominance of strike-slip motion is one of the main characteristics of the Landers earthquake sequence. It indicates that crustal blocks are moving away from the San Andreas fault zone instead of being shortened or extended, to accommodate deformation along the "big bend" in the southern San Andreas fault. The Landers sequence also showed where and how the plate boundary motion is transferred from the southern San Andreas fault into the Eastern California Shear Zone.

Acknowledgments. D. Oppenheimer, M. Rymer, J. Dolan, and two *Journal of Geophysical Research* reviewers, C. Thurber and S. Jaume, provided helpful critical reviews. We thank K. Sieh for stimulating discussions about the tectonics of the Landers earthquake and for providing a map of the surface rupture. We are grateful to the seismic analysts of Caltech and the USGS for quick and competent processing of the earthquake data. This research was partially supported by USGS grant 14-08-0001-G1761 and USGS cooperative agreement 1434-92-A-0960 to Caltech and the Southern California Earthquake Center (SCEC) under NSF cooperative agreement EAR-8920136 and USGS cooperative agreement 14-08-0001-A0899. SCEC publication 54. Contribution 5268, Division of Geological and Planetary Sciences, California Institute of Technology, Pasadena.

REFERENCES

Abercrombie, R. E., J. Mori, and P. C. Leary, Observations of the onset of the 28 June 1992 Landers earthquake: Implications for earthquake nucleation and propagation (abstract), *Eos Trans AGU, 73*, Fall Meeting suppl., 382, 1992.

Bartley, J. M., A. F. Glazner, and E. R. Schermer, North-south contraction of the Mojave Block and strike-slip tectonics in southern California, *Science, 248*, 1398-1401, 1990.

Blewitt, G., M. B. Heflin, K. J. Hurst, D. C. Jefferson, F. H. Webb, and J. F. Zumberge, Absolute far-field displacements from the June 28, 1992, Landers earthquake sequence, *Nature, 361*, 340-342, 1993.

Bortugno, E. J., and T. E. Spittler, Geologic map of the San Bernardino Quadrangle, California, *Map 3A (Geol.)*, scale 1:250,000 edition, Calif. Div. of Mines and Geol., Sacramento, 1986.

DeMets, C., R. G. Gordon, D. F. Argus, and S. Stein, Current plate motions, *Geophys. J. Int., 101*, 425-478, 1990.

Dibblee, T. W., Jr., Areal geology of the western Mojave Desert, California, *U.S. Geol. Surv. Prof. Pap., 522*, 1-153, 1967.

Dokka, R. K., Displacements on late Cenozoic strike-slip faults of the central Mojave Desert, California, *Geology, 11*, 305-308, 1983.

Dokka, R. K., and C. J. Travis, Late Cenozoic strike-slip faulting in the Mojave Desert, California, *Tectonics, 9*, 311-340, 1990a.

Dokka, R. K., and C. J. Travis, Role of the Eastern California Shear Zone in accommodating Pacific-North American plate motion, *Geophys. Res. Lett., 17*, 1323-1326, 1990b.

Eberhart-Phillips, D., L. Hwang, and J. Mori, Preliminary results from the July 1992 seismic calibration experiment along the 1992 Landers rupture (abstract), *Eos Trans. AGU, 73*, Fall Meeting suppl., 382, 1992.

Hadley, D., and H. Kanamori, Seismic structure of the Transverse Ranges, California, *Bull. Geol. Soc. Am., 88*, 1469-1478, 1977.

Harris, R. A., and R. W. Simpson, Changes in static stress on southern California faults after the 1992 Landers earthquake, *Nature, 360*, 251-254, 1992.

Hart, E. W., W. A. Bryant, and J. A. Treiman, Surface faulting associated with the June 1992 Landers earthquake, California, *Calif. Geol., 46*, 10-16, 1993.

Hill, D. P., and et. al, Seismicity in the eastern United States remotely triggered by the *M*7.4 Landers, California, earthquake of June 28, 1992, *Science, 260*, 1617-1623, 1993,.

Hill, R. L., and D. J. Beeby, Surface faulting associated with the 5.2 magnitude Galway Lake earthquake of May 31, 1975: Mojave Desert, San Bernardino County, California, *Geol. Soc. Am. Bull., 88*, 1378-1384, 1977.

Hough, S. E., J. Mori, E. Sembera, G. Glassmoyer, C. Mueller, and S. Lydeen, Southern surface rupture associated with the 6/28/92 M7.4 Landers Earthquake: Did it all happen during the mainshock?, *Geophys. Res. Lett.*, in press, 1993.

Hutton, L. K., C. E. Johnson, J. C. Pechmann, J. E. Ebel, D. W. Given, D. M. Code, and P. T. German, Epicentral locations for the Homestead Valley Earthquake Sequence, March 15, 1979, *Calif. Geol., 33*, 110-114, 1980.

Jennings, C. W., Fault map of California with volcanoes, thermal springs and thermal wells, scale 1:750,000, *geol. data map 1*, Calif. Div. of Mines and Geol., Sacramento, 1975.

Jones, L. M., Foreshocks (1966-1980) in the San Andreas System, California, *Bull. Seismol. Soc. Am., 74*, 1361-1380, 1984.

Jones, L. M., L. K. Hutton, D. D. Given, and C. R. Allen, The North Palm Springs, California, earthquake sequence of July 1986, *Bull. Seismol. Soc. Am., 76*, 1830-1837, 1986.

Kanamori, H., and G. Fuis, Variations of *P*-wave velocity before and after the Galway Lake earthquake (M_L=5.2) and the Goat Mountain earthquakes (M_L=4.7, 4.7) 1975, in the Mojave Desert, California, *Bull. Seismol. Soc. Am., 66*, 2017-2037, 1976.

Kanamori, H., H.-K. Thio, D. Dreger, E. Hauksson, and T. Heaton, Initial investigation of the Landers, California, earthquake of 28 June 1992 using TERRAscope, *Geophys. Res. Lett., 19*, 2267-2270, 1992.

Klein, F. W., User's guide to HYPOINVERSE; A program for VAX and PC350 computers to solve for earthquake locations, *U. S. Geol. Surv. Open File Rep., 85-15*, 24pp., 1985.

Lindh, A., G. Fuis, and C. Mantis, Seismic amplitude measurements suggest foreshocks have different focal mechanisms than aftershocks, *Science, 201*, 56-59, 1978.

Matti, J. C., D. M. Morton, and B. F. Cox, The San Andreas Fault System in the vicinity of the central Transverse Ranges Province, southern California, in *Earthquake Geology San Andreas Fault System Palm Springs to Palmdale, 35th Annual Meeting, Oct. 2-9, 1992*, pp. 13-62, Southern California Section, Association of Engineering Geologists, Los Angeles, 1992.

Meisling, K. E., and R. J. Weldon, Late Cenozoic tectonics of the northwestern San Bernardino Mountains, southern California, *Bull. Geol. Soc. Am., 101*, 106-128, 1989.

Mori, J., and L. M. Jones, Source characteristics and spatial clustering of the foreshocks to the Joshua Tree and Landers earthquakes (abstract), *Eos Trans, AGU, 73*, Fall Meeting suppl., 393, 1992.

Reasenberg, P., and D. Oppenheimer, FPFIT, FPPLOT and FPPAGE: Fortran computer programs for calculating and displaying earthquake fault-plane solutions, *U.S. Geol. Surv. Open File Rep., 85-739*, 109 pp., 1985.

Richter, C. F., C. R. Allen, and J. M. Nordquist, The Desert Hot Springs earthquakes and their tectonic environment, *Bull. Seismol. Soc. Am., 48*, 315-337, 1958.

Roecker, S., and W. L. Ellsworth, VELEST, Fortran program report, *U.S. Geol. Surv.*, 1978.

Rymer, M. J., The 1992 Joshua Tree, California, earthquake: Tectonic setting and triggered slip (abstract), *Eos Trans. AGU, 73*, Fall Meeting suppl., 363, 1992.

Sauber, J., W. Thatcher, and S. C. Solomon, Geodetic measurements of deformation in the central Mojave Desert, California, *J. Geophys. Res., 91*, 12,683-12,693, 1986.

Savage, J. C., M. Lisowski, and W. H. Prescott, An apparent shear zone trending north-northwest across the Mojave Desert into Owens Valley, eastern California, *Geophys. Res. Lett., 17*, 2113-2116, 1990.

Sieh, K., et al., Near-field investigations of the Landers earthquake sequence, April to July 1992, *Science, 260*, 171-176, 1993.

Stein, R. S., G. C. P. King, and J. Lin, Change in failure stress on the San Andreas and surrounding faults caused by the 1992 M=7.4 Landers earthquake, *Science, 258*, 1328-1332, 1992.

Stein, R. S., and M. Lisowski, The 1979 Homestead Valley earthquake sequence, California: Control of aftershocks and postseismic deformation, *J. Geophys. Res., 88*, 6477-6490, 1983.

Sykes, L. R., and L. Seeber, Great earthquakes and great asperities, San Andreas fault, southern California, *Geology, 13*, 835-838, 1985.

Thio, H.-K., and H. Kanamori, A teleseismic study of the Landers earthquake (abstract), *Eos Trans., AGU, 73*, Fall Meeting suppl., 393, 1992.

Treiman, J. A., Eureka Peak and Burnt Mountain Faults. Two "new" faults in Yucca Valley San Bernardino County, California, in *Southern California Section of the Association. of Engineering Geologists, 1992 Field Trip*, edited by D. P. Ebersold, pp. 19-22, Southern California Section of the Association of Engineering Geologists, Los Angeles, 1992.

Utsu, T., A statistical study on the occurrence of aftershocks, *Geophys. Mag.,30*, 521-605, 1961.

Wald, D. J., D. V. Helmberger, H. K. Thio, D. Dreger, and T. H. Heaton, On developing a single rupture model for the 1992 Landers, California, earthquake consistent with static, broadband teleseismic, regional and strong-motion data sets (abstract), *Eos Trans., AGU, 73*, Fall Meeting suppl., 358, 1992.

Webb, T. H., and H. Kanamori, Earthquake focal mechanisms in the eastern Transverse Ranges and San Emigdio Mountains, southern California and evidence for a regional decollement, *Bull. Seismol. Soc. Am., 75*, 737-757, 1985.

Weldon, R. J., and E. Humphreys, A kinematic model of southern California, *Tectonics, 5*, 33-48, 1986.

Williams, P. L., L. R. Sykes, C. Nicholson, and L. Seeber, Seismotectonics of the easternmost Transverse Ranges, California: Relevance for seismic potential of the southern San Andreas Fault, *Tectonics, 9*, 185-204, 1990.

D. Eberhart-Phillips and L. M. Jones, U.S. Geological Survey, 525 S. Wilson Avenue, Pasadena, CA 91106.

E. Hauksson and K. Hutton, Seismological Laboratory, Division of Geological and Planetary Sciences, California Institute of Technology, Pasadena, CA 91125.

(Received April 12, 1993;
revised August 10, 1993;
accepted August 19, 1993.)